Learning Many-Body Hamiltonians with Heisenberg-Limited Scaling

Hsin-Yuan Huang¹, Yu Tong¹, Di Fang, And Yuan Su⁴

¹Institute for Quantum Information and Matter, California Institute of Technology, Pasadena, California 91125, USA

²Department of Mathematics, University of California, Berkeley, California 94720, USA

³Simons Institute for the Theory of Computing, University of California, Berkeley, California 94720, USA

⁴Microsoft Quantum, Redmond, Washington 98052, USA

(Received 3 November 2022; accepted 18 April 2023; published 16 May 2023)

Learning a many-body Hamiltonian from its dynamics is a fundamental problem in physics. In this Letter, we propose the first algorithm to achieve the Heisenberg limit for learning an interacting N-qubit local Hamiltonian. After a total evolution time of $\mathcal{O}(\epsilon^{-1})$, the proposed algorithm can efficiently estimate any parameter in the N-qubit Hamiltonian to ϵ error with high probability. Our algorithm uses ideas from quantum simulation to decouple the unknown N-qubit Hamiltonian H into noninteracting patches and learns H using a quantum-enhanced divide-and-conquer approach. The proposed algorithm is robust against state preparation and measurement error, does not require eigenstates or thermal states, and only uses $\operatorname{polylog}(\epsilon^{-1})$ experiments. In contrast, the best existing algorithms require $\mathcal{O}(\epsilon^{-2})$ experiments and total evolution time. We prove a matching lower bound to establish the asymptotic optimality of our algorithm.

DOI: 10.1103/PhysRevLett.130.200403

Learning an unknown Hamiltonian H from its dynamics $U(t) = e^{-iHt}$ is an important problem that arises in quantum sensing and metrology [1-9], quantum device engineering [10–15], and quantum many-body physics [16–23]. In quantum sensing and metrology, the Hamiltonian Hencodes signals that we want to capture. A more efficient method to learn H implies the ability to extract these signals faster, which could lead to substantial improvement in many applications, such as microscopy, magnetic field sensors, and positioning systems. In quantum computing, learning the unknown Hamiltonian H is crucial for calibrating and engineering the quantum device to design quantum computers with lower error rates. In quantum many-body physics, the unknown Hamiltonian H characterizes the physical system of interest. Obtaining knowledge of H is hence crucial to understanding microscopic physics. A central goal in these applications is to find the most efficient approach for learning H.

In this Letter, we focus on the task of learning many-body Hamiltonians describing a quantum system with a large number of constituents. For concreteness, we consider an N-qubit system with geometrically local interactions. Given any unknown N-qubit geometrically local Hamiltonian H, we can represent H as

$$H = \sum_{a=1}^{M} \lambda_a E_a. \tag{1}$$

Here, $\lambda_1, ..., \lambda_M$ are the unknown parameters and $S = \{E_1, ..., E_M\} \subseteq \{I, X, Y, Z\}^{\otimes N}$ is a subset of *N*-qubit

Pauli operators. Each Pauli operator E_a acts nontrivially on at most $k=\mathcal{O}(1)$ qubits, and each qubit is acted on by $\mathcal{O}(1)$ of the Pauli operators in S. Many-body Hamiltonians with nearest-neighbor interactions on one-dimensional chains, two-dimensional square lattices, and three-dimensional cubic lattices are all special cases of geometrically local Hamiltonians. The goal is to learn the parameters λ_a in the unknown Hamiltonian H. In previous works on learning many-body Hamiltonians [24–35], in order to reach an ϵ precision in estimating the parameters λ_a , the number of experiments and the total time required to evolve the system have a scaling of at least ϵ^{-2} . However, the ϵ^{-2} precision scaling is likely not the best-possible scaling for learning an unknown many-body Hamiltonian H.

In quantum sensing and metrology, the scaling of e^{-2} for learning an unknown parameter to ϵ error is known as the standard quantum limit. For simple classes of Hamiltonians, such as a single-qubit Hamiltonian $H = \omega Z$ with unknown parameter ω , one can surpass the standard quantum limit using quantum-enhanced protocols [1,3,7,36–38]. The true limit set by the basic principles of quantum mechanics is known as the Heisenberg limit, which suggests a scaling of e^{-1} . There are two well-known approaches for achieving the Heisenberg limit for learning $H = \omega Z$. The first approach [3–5] considers evolving a highly entangled state over $\ell = \mathcal{O}(\epsilon^{-1})$ qubits of the system under ℓ parallel Hamiltonian evolutions $(e^{-iHt})^{\otimes \ell}$ with $t = \mathcal{O}(1)$. The second approach [1,39,40] considers long-time coherent evolution $e^{-i\omega tZ}$ with $t = \mathcal{O}(\epsilon^{-1})$ over a single qubit. While the first approach was proposed earlier, the second approach has the advantage of requiring only a single qubit without entanglement.

The e^{-1} scaling underlying the two approaches corresponds to the "total evolution time." If a protocol uses J experiments, where the jth experiment uses the unknown Hamiltonian evolution $e^{-iHt_{j,1}}, ..., e^{-iHt_{j,K_j}}$, then the total evolution time is defined as

$$T \stackrel{\triangle}{=} \sum_{i=1}^{J} \sum_{k=1}^{K_j} t_{j,k}. \tag{2}$$

In the first approach, each experiment uses $\mathcal{O}(\epsilon^{-1})$ constant time Hamiltonian evolutions in parallel, while the second approach uses $\mathcal{O}(\epsilon^{-1})$ constant time Hamiltonian evolutions sequentially resulting in a single long-time evolution. Both quantum sensing approaches result in a total evolution time of $\mathcal{O}(\epsilon^{-1})$.

These quantum-enhanced approaches could be applied to noninteracting systems as studied in multiparameter quantum sensing [41–44]. However, they are challenging to apply in interacting systems with a large system size N and many unknown parameters. The difficulty stems from the many-body interactions in the Hamiltonian H. As time t becomes larger, the entanglement growth in e^{-itH} will cause all the unknown parameters in H to tangle with one another. The many-body entanglement can be seen as a form of decoherence, which kills the quantum enhancement. To prevent the system from becoming too entangled, prior work on learning many-body Hamiltonians focuses on a short-time t, which loses the quantum enhancement and obtains, at best, an e^{-2} scaling.

In this Letter, we propose the first learning algorithm to achieve the Heisenberg limit for learning interacting many-body Hamiltonian. Figure 1 illustrates our algorithm. We prove the following performance guarantee.

Theorem 1: There is an algorithm robust to state preparation and measurement error [45] that achieves the following: For any unknown N-qubit geometrically local Hamiltonian $H = \sum_{a=1}^{M} \lambda_a E_a$ with $|\lambda_a| \leq 1$, after a total evolution time $T = \mathcal{O}(\epsilon^{-1} \log(\delta^{-1}))$, the learning algorithm can obtain estimates $\hat{\lambda}_a$ from the experiments, such that $\Pr[|\hat{\lambda}_a - \lambda_a| \leq \epsilon] \geq 1 - \delta$ for all $a \in \{1, ..., M\}$.

In quantum sensing and metrology, one often considers the standard deviation of the estimate. We can show that to ensure the standard deviation $\sqrt{\mathbb{E}[|\hat{\lambda}_a - \lambda_a|^2]} \leq \epsilon$, we only need a total evolution time of $T = \mathcal{O}(\epsilon^{-1})$. This is because each estimate $\hat{\lambda}_a$ comes from a linear combination of $\mathcal{O}(1)$ eigenvalue estimates through a Hadamard transform, as shown in [[51], Eq. (25)]. Each eigenvalue estimate has standard deviation at most $\mathcal{O}(\epsilon)$ as guaranteed by [[40], Theorem I.1]. Consequently, their linear combination $\hat{\lambda}_a$ also has a standard deviation that scales as $\mathcal{O}(\epsilon)$. Hence, our algorithm saturates the Heisenberg limit in terms of the

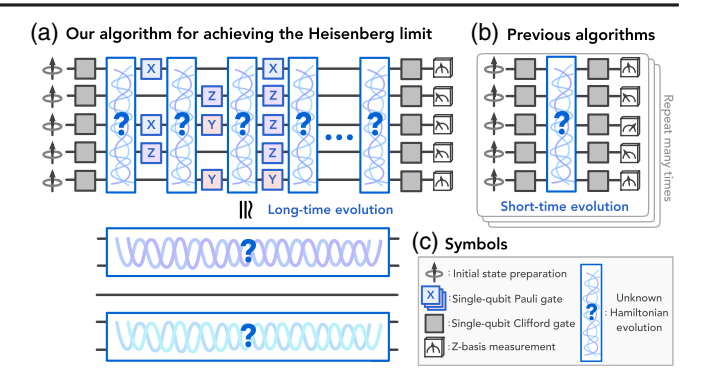


FIG. 1. Algorithms for learning many-body Hamiltonians. (a) Our algorithm for achieving the Heisenberg limit ϵ^{-1} . We perform long-time coherent evolutions interleaved with random Pauli operators. The effective Hamiltonian is decoupled into noninteracting patches and can be efficiently learned. The algorithm only needs $\mathcal{O}(\text{polylog}(\epsilon^{-1}))$ experiments and a total evolution time of $\mathcal{O}(\epsilon^{-1})$. (b) Previous algorithms for achieving the standard quantum limit ϵ^{-2} . Previous methods [26,29,33,34] repeatedly run a short-time evolution for many times. One needs $\mathcal{O}(\epsilon^{-2})$ experiments and a total evolution time of $\mathcal{O}(\epsilon^{-2})$. (c) Symbols: The symbols used in (a), (b). The unknown Hamiltonian evolution is $U(t) = e^{-iHt}$.

standard deviation. Our algorithm has the additional advantage of not requiring eigenstates or thermal states of the Hamiltonian H. Each of our experiments consists of the preparation of a noisy all-zero state $|0^N\rangle$, the evolution under the Hamiltonian H interleaved with single-qubit Clifford gates, and a noisy Z-basis measurement. The total number of experiments is only $\mathcal{O}(\text{polylog}(\varepsilon^{-1}))$, which is significantly smaller than $\Theta(\varepsilon^{-1})$. After running the experiments, the classical computational time to estimate all parameters is only $\mathcal{O}(N\text{polylog}(\varepsilon^{-1}))$. Detailed statements can be found in [[51], Theorems 13 and 21]. We note that our result generalizes to all low-intersection Hamiltonians as given in [[51], Definition 2].

To establish the optimality of the proposed algorithm, we prove a matching lower bound.

Theorem 2: Suppose there is a learning algorithm robust to state preparation and measurement error that achieves the following. For any unknown N-qubit geometrically local Hamiltonian $H = \sum_{a=1}^M \lambda_a E_a$ with $|\lambda_a| \leq 1$, after a total evolution time T, the learning algorithm can obtain estimates $\hat{\lambda}_a$ from the experiments, such that $\Pr[|\hat{\lambda}_a - \lambda_a| \leq \epsilon] \geq 1 - \delta$ for all $a \in \{1, ..., M\}$. Then, $T = \Omega(\epsilon^{-1} \log(\delta^{-1}))$.

Thus, there is no algorithm that can perform asymptotically better than the one given in Theorem 1. Moreover, the lower bound can be seen as an algorithmic proof of the Heisenberg limit with the failure probability δ taken into account. It holds not only for algorithms with a fixed set of experiments but also for adaptive experiments that use information from previous experiment outcomes, following the setup in [52–55].

In the following, we provide the ideas for designing the proposed learning algorithm and establishing the proof of the main results. All parts except for the last are devoted to Theorem 1. The last part is Theorem 2.

Reshaping an unknown Hamiltonian.—A key technique used throughout the design of our learning algorithm is the idea of reshaping an unknown Hamiltonian using Hamiltonian simulation techniques. Recall that given a set of Hamiltonians H_1, \ldots, H_K and the ability to implement the unitaries $e^{-itH_1}, \ldots, e^{-itH_K}$, many Hamiltonian simulation techniques allow one to approximately implement the unitary $e^{-it}\sum_{k=1}^K H_k$. Note that these approximation formulas are valid for unitaries and no knowledge of the underlying Hamiltonian is required. As such, they are applicable to the learning problem considered here.

For example, a randomized Hamiltonian simulation algorithm known as qDRIFT [56–58] considers an approximation (as a quantum channel) given by

$$e^{-it\sum_{k=1}^{K}H_k} \approx e^{-i(t/r)H_{k_r}}...e^{-i(t/r)H_{k_1}},$$
 (3)

where r is an integer that sets the approximation error, $k_1, ..., k_r$ are independent random variables sampled according to some probability distribution over $\{1, ..., K\}$. Alternatively, we can also use the second-order Trotterization method [59–61] in our algorithm to reduce the asymptotic scaling of the number of Clifford gates required. Higher-order Trotterizations are not used because they require evolving backward in time.

Now, consider the unknown N-qubit Hamiltonian H that we hope to learn. We want to reshape it into the following Hamiltonian to facilitate learning:

$$\tilde{H} \stackrel{\triangle}{=} \sum_{k=1}^{K} w_k H_k, \tag{4}$$

where $H_k \stackrel{\triangle}{=} w_k U_k H U_k^{\dagger}$ and U_k is a unitary for each k = 1, 2, ..., K. The weights $w_k \ge 0$. Any choice of unitaries U_k and weights w_k can be used. Later, to achieve the Heisenberg limit, we will choose specific U_k and w_k to ensure \tilde{H} disentangles the many-body system into noninteracting patches involving few qubits and has known eigenvectors irrespective of what H is. Our choice for each U_k will be a tensor product of Pauli operators. Using either qDRIFT or Trotterization, we only need to implement e^{-iH_k} , which can be done through $e^{-iH_kt} = U_k e^{-i(w_kt)H} U_k^{\dagger}$. To be more specific, we can implement e^{-iH_Kt} by first applying the unitary U_k^\dagger , letting the system evolve for time $w_k t$, and then applying U_k . Using Hamiltonian simulation techniques, we can evolve under the N-qubit unitary $e^{-it\tilde{H}}$. This reshaping technique is related to experimental approaches for engineering Hamiltonians through pulse sequences or strong fields [62–68]. Similar ideas have also been used to project H into the quantum Zeno subspace [69,70]. The reshaping will lead to a small approximation error, which we discuss later (for a detailed discussion, see [51], Sec. IV and VI]).

Learning a few-qubit Hamiltonian.—We now show how the Hamiltonian reshaping technique is useful in learning Hamiltonians. We begin with a simple question: how can one learn a few-qubit Hamiltonian on $\mathcal{O}(1)$ qubits with Heisenberg-limited precision scaling? If we naively apply quantum process tomography [54,71–77] to learn the unknown Hamiltonian, we would have an ϵ^{-2} dependence in the number of measurements needed, where ϵ is the desired precision of the Hamiltonian parameters. Current methods with a Heisenberg-limited scaling typically require the Hamiltonian to be of a simple form, e.g., $H = \lambda X$ [1–9,39,40]. Therefore we need to consider a different method.

We show that for a few-qubit Hamiltonian we can learn all the parameters involved using $\mathcal{O}(\epsilon^{-1}\log(\delta^{-1}))$ total evolution time, and $\mathcal{O}(\text{polylog}(\epsilon^{-1})\log(\delta^{-1}))$ number of experiments. As an example, let us consider an arbitrary two-qubit Hamiltonian,

$$H = \sum_{P,P' \in \{I,X,Y,Z\}} \lambda_{PP'} P \otimes P', \tag{5}$$

with $|\lambda_{PP'}| \le 1$. Suppose we want to estimate the parameter λ_{XZ} . Then we can consider reshaping the unknown Hamiltonian H using $U_1 = I$, $U_2 = X_1$, $U_3 = Z_2$, $U_4 = X_1Z_2$, and $w_1 = w_2 = w_3 = w_4 = \frac{1}{4}$. The new unknown Hamiltonian, after reshaping, is given by

$$\tilde{H} \stackrel{\triangle}{=} \frac{1}{4} (H + X_1 H X_1 + Z_2 H Z_2 + X_1 Z_2 H X_1 Z_2)
= \lambda_{XZ} X_1 Z_2 + \lambda_{XI} X_1 + \lambda_{IZ} Z_2.$$
(6)

The second equality is because the linear combination over the four terms eliminates all Pauli terms in *H* that do not have *I* or *X* on the first qubit and *I* or *Z* on the second qubit.

This new unknown Hamiltonian \tilde{H} gives us one crucial advantage: we have access to its eigenstates. This is because in \tilde{H} , for each qubit, there is only one (nonidentity) Pauli operator associated with it. The eigenbasis for the new unknown Hamiltonian \tilde{H} is always given by $\{|+\rangle|0\rangle, |+\rangle|1\rangle, |-\rangle|0\rangle, |-\rangle|1\rangle\}$ regardless of the values of the unknown coefficients. We can use this information, together with the robust phase estimation algorithm in [40], to estimate the differences between pairs of eigenvalues, which in turn yield the parameters $\lambda_{XZ}, \lambda_{XI}, \lambda_{IZ}$ through a Hadamard transform. The procedure for applying random Pauli operators and obtaining parameters from eigenvalue estimation is described in detail in [[51], Sec. II.B and III.B]. By using different choices of U_1, \ldots, U_4 to reshape H, we can get all the parameters $\lambda_{PP'}$ in the two-qubit

Hamiltonian H. The same idea generalizes to arbitrary Hamiltonians on $\mathcal{O}(1)$ qubits.

Learning a many-qubit Hamiltonian through divide and conquer.—If we want to learn a many-qubit Hamiltonian by directly applying the above method, the total evolution time will scale exponentially with the number of qubits. Here, we present a divide-and-conquer approach to address this problem. To illustrate the proposed approach, let us consider a simple example of an inhomogeneous Heisenberg model on *N* qubit with a Hamiltonian given by

$$H = \sum_{\alpha=1}^{N-1} \left(\lambda_x^{\alpha} X_{\alpha} X_{\alpha+1} + \lambda_y^{\alpha} Y_{\alpha} Y_{\alpha+1} + \lambda_z^{\alpha} Z_{\alpha} Z_{\alpha+1} \right), \quad (7)$$

where λ_x^{α} , λ_y^{α} , λ_z^{α} are the unknown parameters, and X_{α} , Y_{α} , Z_{α} are the Pauli operators acting on qubit α . Suppose we want to learn the parameter λ_x^1 on the first two qubits. In order to achieve this, we reshape the unknown Hamiltonian H with $U_1 = I$, $U_2 = X_3$, $U_3 = Y_3$, $U_4 = Z_3$, and $w_1 = w_2 = w_3 = w_4 = \frac{1}{4}$. The new unknown Hamiltonian after the reshaping is given by

$$\tilde{H} = \frac{1}{4} (H + X_3 H X_3 + Y_3 H Y_3 + Z_3 H Z_3)$$

$$= \tilde{H}_{1,2} + \tilde{H}_{>4}, \tag{8}$$

where

$$\tilde{H}_{1,2} = \lambda_x^{1,2} X_1 X_2 + \lambda_x^{1,2} Y_1 Y_2 + \lambda_x^{1,2} Z_1 Z_2 \tag{9}$$

and $\tilde{H}_{\geq 4}$ only contains terms acting on qubits 4, 5, ..., N. The second equality in Eq. (8) holds for the following reason: for each Pauli operator $P \in \{I, X, Y, Z\}^{\otimes N}$, if it acts nontrivially on the third qubit, then we can show that

$$\frac{1}{4}(P + X_3PX_3 + Y_3PY_3 + Z_3PZ_3) = 0.$$
 (10)

On the other hand, for Pauli operator P that acts as identity on the third qubit, we can show that

$$\frac{1}{4}(P + X_3PX_3 + Y_3PY_3 + Z_3PZ_3) = P.$$
 (11)

Therefore from Eq. (8), after the reshaping, the new Hamiltonian \tilde{H} does not generate entanglement between qubits 1,2 and the rest of the system, and these two qubits evolve under the Hamiltonian $\tilde{H}_{1,2}$. This enables us to apply the learning algorithm for few-qubit Hamiltonians to $\tilde{H}_{1,2}$ to estimate λ_1^1 .

We can apply the above idea to learn every parameter in the Hamiltonian with a number of experiments that scales linearly in the system size N rather than exponential in N. We show that one could do better than linear scaling by a

parallelization technique. In particular, we discuss how one could learn all the parameters $\lambda_x^1, \lambda_x^4, \lambda_x^7, \cdots$ in parallel. Consider reshaping the unknown N-qubit Hamiltonian H given in Eq. (7) using $U_1 = I$, $U_2 = X_3X_6X_9...$, $U_3 = Y_3Y_6Y_9...$, $U_4 = Z_3Z_6Z_9...$, and $w_1 = w_2 = w_3 = w_4 = 1/4$. Then the new Hamiltonian under reshaping is given by $\tilde{H} = \tilde{H}_{1,2} + \tilde{H}_{4,5} + \tilde{H}_{7,8} + \cdots$, where $\tilde{H}_{\alpha,\alpha+1}$ is supported on qubits α and $\alpha+1$ for all $\alpha=1,4,7,...$ Using a reshaping based on four unitaries $U_1,...,U_4$, we have turned the unknown N-qubit interacting Hamiltonian H into a new Hamiltonian \tilde{H} with many noninteracting patches of two qubits. Each two-qubit patch is now evolving independently from the others. This decoupling enables us to estimate the parameters in parallel using the algorithm for learning few-qubit Hamiltonians.

This divide-and-conquer method works for any local Hamiltonian defined in Eq. (1). For this more general class of Hamiltonians, we determine how the reshaping is done by performing a coloring over its cluster interaction graph (a graph consisting of clusters of qubits that are acted on by a Pauli term in the Hamiltonian) [[51], Lemma 5]. The coloring enables us to choose qubits, on which we apply random I, X, Y, Z operators to decouple clusters of the same color from each other, thus enabling parallel estimation of the parameters associated with these clusters. For details, see [[51], Sec. I.B, II, and V]. A complete description of our algorithm for general local Hamiltonians can be found in [[51], Algorithm 2]. The cost of the algorithm is summarized in [[51], Theorems 13 and 21] (for the randomization and Trotterization approaches, respectively).

Characterizing approximation error in reshaping Hamiltonians.—The estimation error of the proposed learning algorithm depends on the quantum measurement error as well as the approximation error when we reshape the unknown Hamiltonian into other forms. One way to analyze the approximation error is through the error analysis considered in [56] if we use qDRIFT to reshape or in [78] when using the second-order Trotter formula. However, these analyses are concerned with the error in the worst-case scenario over all possible input states and all observables. For the learning task given here, it leads to an overestimation of the approximation error as some key properties of the problem are not incorporated.

Consider the example of learning an inhomogeneous Heisenberg model on N qubits given in the previous section. To evolve under the N-qubit Hamiltonian reshaped \tilde{H} for time t, the analysis in [56] shows that the approximation error of qDRIFT with r steps is given by $\mathcal{O}(N^2t^2/r)$. Here, \tilde{H} is decoupled into many two-qubit patches that do not interact with each other, which prevents errors from propagating across the entire N-qubit system. We are interested only in the accuracy of evolving each patch, and the error from elsewhere in the system should not affect estimations of local observables. Similar considerations have been used to improve the error analysis of Hamiltonian simulation

methods based on observable and initial state information [79–83]. In our case, a tighter analysis [84] using these facts shows that the approximation error is given by $\mathcal{O}(t^2/r)$ without an N dependence. We give the improved analysis for reshaping Hamiltonians using the randomization approach in [51], Sec. IV]. The improved analysis for using the second-order Trotter formula is given in [51], Sec. VI].

Establishing a matching lower bound.—We prove a matching lower bound of $T = \Omega(\epsilon^{-1} \log(\delta^{-1}))$ on the total evolution time T [86]. The optimality with respect to the ϵ dependence is obtained by the Heisenberg limit. However, the optimality with respect to the failure probability δ has not been proven in the literature. We consider any learning algorithm that can run new experiments based adaptively on the outcomes of previous experiments. In order to handle adaptivity, we consider the rooted tree representation of the learning algorithm [53,55], and consider the task of distinguishing between two distinct Hamiltonians $H_+ = \pm \epsilon Z$.

We begin by considering how well one could use a single experiment to distinguish H_{\pm} , which is characterized by the total variation (TV) distance between the probability distribution over experimental outcomes under H_{\pm} . We characterize the TV distance in a single experiment. Then we consider an induction over every subtree of the learning algorithm to establish the TV distance over multiple experiments. A central technique is to control how each additional experiment improves one's ability to distinguish H_{\pm} . The proof of the lower bound is given in [[51], Sec. VII].

Discussion.—Our work shows that the Heisenberg limit can be achieved in the task of learning a large class of many-body local Hamiltonians with many unknown parameters. On the theoretical side, the central open question is whether our result can be extended to learning other classes of many-body Hamiltonians. For example, in an N-qubit Hamiltonian with all-to-all two-body interactions, our techniques achieve the Heisenberg limit with a quadratic dependence on system size N by learning all pairwise interactions one by one. This gives rise to the following question: can we achieve a scaling of T = $\mathcal{O}(\epsilon^{-1}\log(\delta^{-1}))$ for N-qubit Hamiltonians with all-to-all interactions? In addition to the above example, can we achieve the Heisenberg limit for learning fermionic or bosonic many-body Hamiltonians? Answering these questions is important for applications such as reconstructing the structure of large molecules or learning the interactions in an exotic quantum material. Even more ambitiously, can one achieve the above scaling for learning the unknown parameters in an arbitrary N-qubit Hamiltonian without any structure? On the practical side, the central question is how to achieve the Heisenberg limit with minimal controllable quantum operations. For example, could one achieve the scaling $T = \mathcal{O}(\epsilon^{-1} \log(\delta^{-1}))$ for learning N-qubit local Hamiltonian H in a restricted model where we cannot interleave the unknown Hamiltonian evolution with single-qubit gates and can only control state preparation and measurement? Understanding these questions will be crucial for physically achieving the Heisenberg limit in learning many-body Hamiltonians.

The authors thank Matthias Caro, Richard Kueng, Lin Lin, Jarrod McClean, Praneeth Netrapalli, and John Preskill for valuable input and inspiring discussions. H.-Y. H. is supported by a Google Ph.D. fellowship and a MediaTek Research Young Scholarship. Y. T. is supported in part by the U.S. Department of Energy Office of Science (DE-SC0019374), Office of Advanced Scientific Computing Research (DE-SC0020290), Office of High Energy Physics (DE-ACO2-07CH11359), and under the Quantum System Accelerator project. Work supported by DE-SC0020290 is supported by the DOE QuantISED program through the theory consortium "Intersections of QIS and Theoretical Particle Physics" at Fermilab. The Institute for Quantum Information and Matter is a NSF Physics Frontiers Center. D. F. is supported by NSF Quantum Leap Challenge Institute (QLCI) program under Grant No. OMA-2016245, NSF DMS-2208416, and a grant from the Simons Foundation under Grant No. 825053.

H.-Y. H. and Y. T. contributed equally to this work.

- [1] M. de Burgh and S. D. Bartlett, Quantum methods for clock synchronization: Beating the standard quantum limit without entanglement, Phys. Rev. A 72, 042301 (2005).
- [2] A. Valencia, G. Scarcelli, and Y. Shih, Distant clock synchronization using entangled photon pairs, Appl. Phys. Lett. 85, 2655 (2004).
- [3] D. Leibfried, M. D. Barrett, T. Schaetz, J. Britton, J. Chiaverini, W. M. Itano, J. D. Jost, C. Langer, and D. J. Wineland, Toward Heisenberg-limited spectroscopy with multiparticle entangled states, Science 304, 1476 (2004).
- [4] J. J. Bollinger, W. M. Itano, D. J. Wineland, and D. J. Heinzen, Optimal frequency measurements with maximally correlated states, Phys. Rev. A 54, R4649 (1996).
- [5] H. Lee, P. Kok, and J. P. Dowling, A quantum Rosetta stone for interferometry, J. Mod. Opt. **49**, 2325 (2002).
- [6] K. McKenzie, D. A. Shaddock, D. E. McClelland, B. C. Buchler, and P. K. Lam, Experimental Demonstration of a Squeezing-Enhanced Power-Recycled Michelson Interferometer for Gravitational Wave Detection, Phys. Rev. Lett. 88, 231102 (2002).
- [7] M. J. Holland and K. Burnett, Interferometric Detection of Optical Phase Shifts at the Heisenberg Limit, Phys. Rev. Lett. 71, 1355 (1993).
- [8] D. J. Wineland, J. J. Bollinger, W. M. Itano, F. L. Moore, and D. J. Heinzen, Spin squeezing and reduced quantum noise in spectroscopy, Phys. Rev. A 46, R6797 (1992).
- [9] C. M. Caves, Quantum-mechanical noise in an interferometer, Phys. Rev. D 23, 1693 (1981).
- [10] N. Boulant, T.F. Havel, M. A. Pravia, and D. G. Cory, Robust method for estimating the Lindblad operators of a dissipative quantum process from measurements of the

- density operator at multiple time points, Phys. Rev. A **67**, 042322 (2003).
- [11] L. Innocenti, L. Banchi, A. Ferraro, S. Bose, and M. Paternostro, Supervised learning of time-independent Hamiltonians for gate design, New J. Phys. 22, 065001 (2020).
- [12] E. Ben Av, Y. Shapira, N. Akerman, and R. Ozeri, Direct reconstruction of the quantum-master-equation dynamics of a trapped-ion qubit, Phys. Rev. A 101, 062305 (2020).
- [13] M. D. Shulman, S. P. Harvey, J. M. Nichol, S. D. Bartlett, A. C. Doherty, V. Umansky, and A. Yacoby, Suppressing qubit dephasing using real-time Hamiltonian estimation, Nat. Commun. 5, 5156 (2014).
- [14] S. Sheldon, E. Magesan, J. M. Chow, and J. M. Gambetta, Procedure for systematically tuning up cross-talk in the cross-resonance gate, Phys. Rev. A 93, 060302(R) (2016).
- [15] N. Sundaresan, I. Lauer, E. Pritchett, E. Magesan, P. Jurcevic, and J. M. Gambetta, Reducing unitary and spectator errors in cross resonance with optimized rotary echoes, PRX Quantum 1, 020318 (2020).
- [16] N. Wiebe, C. Granade, C. Ferrie, and D. Cory, Quantum Hamiltonian learning using imperfect quantum resources, Phys. Rev. A 89, 042314 (2014).
- [17] N. Wiebe, C. Granade, C. Ferrie, and D. G. Cory, Hamiltonian Learning and Certification Using Quantum Resources, Phys. Rev. Lett. **112**, 190501 (2014).
- [18] G. Verdon, J. Marks, S. Nanda, S. Leichenauer, and J. Hidary, Quantum hamiltonian-based models and the variational quantum thermalizer algorithm, arXiv:1910.02071.
- [19] D. Burgarth and A. Ajoy, Evolution-Free Hamiltonian Parameter Estimation through Zeeman Markers, Phys. Rev. Lett. **119**, 030402 (2017).
- [20] J. Wang, S. Paesani, R. Santagati, S. Knauer, A. A. Gentile, N. Wiebe, M. Petruzzella, J. L. O'Brien, J. G. Rarity, A. Laing *et al.*, Experimental quantum Hamiltonian learning, Nat. Phys. 13, 551 (2017).
- [21] H. Y. Kwon, H. G. Yoon, C. Lee, G. Chen, K. Liu, A. K. Schmid, Y. Z. Wu, J. W. Choi, and C. Won, Magnetic Hamiltonian parameter estimation using deep learning techniques, Sci. Adv. 6, eabb0872 (2020).
- [22] D. Wang, S. Wei, A. Yuan, F. Tian, K. Cao, Q. Zhao, Y. Zhang, C. Zhou, X. Song, D. Xue, and S. Yang, Machine learning magnetic parameters from spin configurations, Adv. Sci. 7, 2000566 (2020).
- [23] H.-Y. Huang, R. Kueng, and J. Preskill, Predicting many properties of a quantum system from very few measurements, Nat. Phys. **16**, 1050 (2020).
- [24] Z. Li, L. Zou, and T. H. Hsieh, Hamiltonian Tomography via Quantum Quench, Phys. Rev. Lett. **124**, 160502 (2020).
- [25] L. Che, C. Wei, Y. Huang, D. Zhao, S. Xue, X. Nie, J. Li, D. Lu, and T. Xin, Learning quantum Hamiltonians from single-qubit measurements, Phys. Rev. Res. 3, 023246 (2021).
- [26] J. Haah, R. Kothari, and E. Tang, Optimal learning of quantum Hamiltonians from high-temperature gibbs states, arXiv:2108.04842.
- [27] W. Yu, J. Sun, Z. Han, and X. Yuan, Practical and efficient Hamiltonian learning, arXiv:2201.00190.
- [28] D. Hangleiter, I. Roth, J. Eisert, and P. Roushan, Precise Hamiltonian identification of a superconducting quantum processor, arXiv:2108.08319.

- [29] D. S. Franca, L. A. Markovich, V. Dobrovitski, A. H. Werner, and J. Borregaard, Efficient and robust estimation of many-qubit Hamiltonians, arXiv:2205.09567.
- [30] A. Zubida, E. Yitzhaki, N. H. Lindner, and E. Bairey, Optimal short-time measurements for Hamiltonian learning, arXiv:2108.08824.
- [31] E. Bairey, I. Arad, and N. H. Lindner, Learning a Local Hamiltonian from Local Measurements, Phys. Rev. Lett. **122**, 020504 (2019).
- [32] C. E. Granade, C. Ferrie, N. Wiebe, and D. G. Cory, Robust online Hamiltonian learning, New J. Phys. **14**, 103013 (2012).
- [33] A. Gu, L. Cincio, and P.J. Coles, Practical black box Hamiltonian learning, arXiv:2206.15464.
- [34] F. Wilde, A. Kshetrimayum, I. Roth, D. Hangleiter, R. Sweke, and J. Eisert, Scalably learning quantum many-body Hamiltonians from dynamical data (2022).
- [35] S. Krastanov, S. Zhou, S. T. Flammia, and L. Jiang, Stochastic estimation of dynamical variables, Quantum Sci. Technol. 4, 035003 (2019).
- [36] V. Giovannetti, S. Lloyd, and L. Maccone, Advances in quantum metrology, Nat. Photonics 5, 222 (2011).
- [37] S. Zhou, M. Zhang, J. Preskill, and L. Jiang, Achieving the Heisenberg limit in quantum metrology using quantum error correction, Nat. Commun. 9, 78 (2017).
- [38] C. L. Degen, F. Reinhard, and P. Cappellaro, Quantum sensing, Rev. Mod. Phys. 89, 035002 (2017).
- [39] B. L. Higgins, D. W. Berry, S. D. Bartlett, H. M. Wiseman, and G. J. Pryde, Entanglement-free Heisenberg-limited phase estimation, Nature (London) **450**, 393 (2007).
- [40] S. Kimmel, G. H. Low, and T. J. Yoder, Robust calibration of a universal single-qubit gate set via robust phase estimation, Phys. Rev. A **92**, 062315 (2015).
- [41] M. Skotiniotis, P. Sekatski, and W. Dür, Quantum metrology for the Ising Hamiltonian with transverse magnetic field, New J. Phys. **17**, 073032 (2015).
- [42] S. Ragy, M. Jarzyna, and R. Demkowicz-Dobrzański, Compatibility in multiparameter quantum metrology, Phys. Rev. A 94, 052108 (2016).
- [43] M. Gessner, L. Pezzè, and A. Smerzi, Sensitivity Bounds for Multiparameter Quantum Metrology, Phys. Rev. Lett. 121, 130503 (2018).
- [44] I. Apellaniz, I. Urizar-Lanz, Z. Zimborás, P. Hyllus, and G. Tóth, Precision bounds for gradient magnetometry with atomic ensembles, Phys. Rev. A 97, 053603 (2018).
- [45] See [46–51] for more detailed discussion on SPAM-robustness.
- [46] E. Knill, D. Leibfried, R. Reichle, J. Britton, R. B. Blakestad, J. D. Jost, C. Langer, R. Ozeri, S. Seidelin, and D. J. Wineland, Randomized benchmarking of quantum gates, Phys. Rev. A 77, 012307 (2008).
- [47] E. Magesan, J. M. Gambetta, and J. Emerson, Scalable and Robust Randomized Benchmarking of Quantum Processes, Phys. Rev. Lett. 106, 180504 (2011).
- [48] A. Erhard, J. J. Wallman, L. Postler, M. Meth, R. Stricker, E. A. Martinez, P. Schindler, T. Monz, J. Emerson, and R. Blatt, Characterizing large-scale quantum computers via cycle benchmarking, Nat. Commun. 10, 1 (2019).
- [49] R. Harper, S. T. Flammia, and J. J. Wallman, Efficient learning of quantum noise, Nat. Phys. **16**, 1184 (2020).

- [50] A. Elben, S. T. Flammia, H.-Y. Huang, R. Kueng, J. Preskill, B. Vermersch, and P. Zoller, The randomized measurement toolbox, Nat. Rev. Phys. 5, 9 (2023).
- [51] See Supplemental Material at http://link.aps.org/ supplemental/10.1103/PhysRevLett.130.200403 for details of our algorithm and the proof of the main results.
- [52] D. Aharonov, J. Cotler, and X.-L. Qi, Quantum algorithmic measurement, Nat. Commun. 13, 1 (2022).
- [53] S. Chen, J. Cotler, H.-Y. Huang, and J. Li, Exponential separations between learning with and without quantum memory, in *Proceedings of 2021 IEEE 62nd Annual Symposium on Foundations of Computer Science (FOCS)* (IEEE, New York, 2022), pp. 574–585.
- [54] H.-Y. Huang, S. T. Flammia, and J. Preskill, Foundations for learning from noisy quantum experiments, arXiv:2204 .13691.
- [55] H.-Y. Huang, M. Broughton, J. Cotler, S. Chen, J. Li, M. Mohseni, H. Neven, R. Babbush, R. Kueng, J. Preskill *et al.*, Quantum advantage in learning from experiments, Science 376, 1182 (2022).
- [56] E. Campbell, Random Compiler for Fast Hamiltonian Simulation, Phys. Rev. Lett. 123, 070503 (2019).
- [57] D. W. Berry, A. M. Childs, Y. Su, X. Wang, and N. Wiebe, Time-dependent Hamiltonian simulation with L¹-norm scaling, Quantum 4, 254 (2020).
- [58] C.-F. Chen, H.-Y. Huang, R. Kueng, and J. A. Tropp, Concentration for random product formulas, PRX Quantum 2, 040305 (2021).
- [59] M. Suzuki, General theory of fractal path integrals with applications to manybody theories and statistical physics, J. Math. Phys. (N.Y.) **32**, 400 (1991).
- [60] S. Lloyd, Universal quantum simulators, Science **273**, 1073 (1996).
- [61] D. W. Berry, G. Ahokas, R. Cleve, and B. C. Sanders, Efficient quantum algorithms for simulating sparse Hamiltonians, Commun. Math. Phys. 270, 359 (2007).
- [62] L. Viola, E. Knill, and S. Lloyd, Dynamical Decoupling of Open Quantum Systems, Phys. Rev. Lett. 82, 2417 (1999).
- [63] K. Khodjasteh and D. A. Lidar, Performance of deterministic dynamical decoupling schemes: Concatenated and periodic pulse sequences, Phys. Rev. A 75, 062310 (2007).
- [64] A. Ajoy and P. Cappellaro, Quantum Simulation via Filtered Hamiltonian Engineering: Application to Perfect Quantum Transport in Spin Networks, Phys. Rev. Lett. 110, 220503 (2013).
- [65] G. T. Genov and N. V. Vitanov, Dynamical Suppression of Unwanted Transitions in Multistate Quantum Systems, Phys. Rev. Lett. 110, 133002 (2013).
- [66] A. Stark, N. Aharon, T. Unden, D. Louzon, A. Huck, A. Retzker, U. L. Andersen, and F. Jelezko, Narrow-bandwidth sensing of high-frequency fields with continuous dynamical decoupling, Nat. Commun. 8, 1 (2017).
- [67] S. Schmitt, T. Gefen, F. M. Stürner, T. Unden, G. Wolff, C. Müller, J. Scheuer, B. Naydenov, M. Markham, S. Pezzagna, J. Meijer, I. Schwarz, M. Plenio, A. Retzker, L. P. McGuinness, and F. Jelezko, Submillihertz magnetic spectroscopy performed with a nanoscale quantum sensor, Science 356, 832 (2017).
- [68] S. Schmitt, T. Gefen, D. Louzon, C. Osterkamp, N. Staudenmaier, J. Lang, M. Markham, A. Retzker,

- L. P. McGuinness, and F. Jelezko, Optimal frequency measurements with quantum probes, npj Quantum Inf. 7, 1 (2021).
- [69] M. C. Tran, Y. Su, D. Carney, and J. M. Taylor, Faster digital quantum simulation by symmetry protection, PRX Quantum 2, 010323 (2021).
- [70] D. Burgarth, P. Facchi, G. Gramegna, and K. Yuasa, One bound to rule them all: From Adiabatic to Zeno, Quantum 6, 737 (2022).
- [71] M. Mohseni, A. T. Rezakhani, and D. A. Lidar, Quantum-process tomography: Resource analysis of different strategies, Phys. Rev. A 77, 032322 (2008).
- [72] A. J. Scott, Optimizing quantum process tomography with unitary 2-designs, J. Phys. A 41, 055308 (2008).
- [73] J. L. O'Brien, G. J. Pryde, A. Gilchrist, D. F. V. James, N. K. Langford, T. C. Ralph, and A. G. White, Quantum Process Tomography of a Controlled-Not Gate, Phys. Rev. Lett. 93, 080502 (2004).
- [74] R. Levy, D. Luo, and B. K. Clark, Classical shadows for quantum process tomography on near-term quantum computers, arXiv:2110.02965.
- [75] S. T. Merkel, J. M. Gambetta, J. A. Smolin, S. Poletto, A. D. Córcoles, B. R. Johnson, C. A. Ryan, and M. Steffen, Self-consistent quantum process tomography, Phys. Rev. A 87, 062119 (2013).
- [76] E. Nielsen, J. K. Gamble, K. Rudinger, T. Scholten, K. Young, and R. Blume-Kohout, Gate set tomography, Quantum 5, 557 (2021).
- [77] R. Blume-Kohout, J. K. Gamble, E. Nielsen, K. Rudinger, J. Mizrahi, K. Fortier, and P. Maunz, Demonstration of qubit operations below a rigorous fault tolerance threshold with gate set tomography, Nat. Commun. 8, 1 (2017).
- [78] A. M. Childs, Y. Su, M. C. Tran, N. Wiebe, and S. Zhu, Theory of Trotter Error with Commutator Scaling, Phys. Rev. X 11, 011020 (2021).
- [79] B. Şahinoğlu and R. D. Somma, Hamiltonian simulation in the low-energy subspace, npj Quantum Inf. 7, 1 (2021).
- [80] Y. Su, H.-Y. Huang, and E. T. Campbell, Nearly tight trotterization of interacting electrons, Quantum 5, 495 (2021).
- [81] D. An, D. Fang, and L. Lin, Time-dependent unbounded Hamiltonian simulation with vector norm scaling, Quantum 5, 459 (2021).
- [82] Y. Borns-Weil and D. Fang, Uniform observable error bounds of trotter formulae for the semiclassical Schrödinger equation, arXiv:2208.07957.
- [83] Y. Tong, V. V. Albert, J. R. McClean, J. Preskill, and Y. Su, Provably accurate simulation of gauge theories and bosonic systems, Quantum 6, 816 (2022).
- [84] We use methods in [85] to obtain long-time evolution error bounds from short-time evolution error bounds.
- [85] R. J. LeVeque, Finite difference Methods for Ordinary and Partial Differential Equations: Steady-State and Time-Dependent Problems (SIAM, Philadelphia, 2007).
- [86] The proof uses results in [87,88] and other works listed in the Supplemental Material thesupplement.
- [87] I. Nechita, Z. Puchała, Ł. Pawela, and K. Życzkowski, Almost all quantum channels are equidistant, J. Math. Phys. (N.Y.) **59**, 052201 (2018).
- [88] J. Watrous, *The Theory of Quantum Information* (Cambridge University Press, Cambridge, England, 2018).

Supplementary material for $Learning\ many-body\ Hamiltonians\ with$ $Heisenberg-limited\ scaling$

Hsin-Yuan Huang, 1 Yu
 ${\rm Tong}, ^{1,\, 2}$ Di ${\rm Fang}, ^{2,\, 3}$ and Yuan ${\rm Su}^4$

¹Institute for Quantum information and Matter, California Institute of Technology

²Department of Mathematics, University of California, Berkeley

³Simons Institute for the Theory of Computing, University of California, Berkeley

⁴Microsoft Quantum

(Dated: March 11, 2023)

CONTENTS

I.	Preliminaries	2
	A. Notations	2
	B. Hamiltonians	2
II.	Reshaping Hamiltonians using randomization	3
	A. Decoupling into noninteracting patches	3
	B. Isolating the diagonal Hamiltonian	4
	C. Combining the two reshaping procedures	5
III.	Learning the unknown Hamiltonian after reshaping	6
	A. Executing quantum experiments	6
	B. Estimating the diagonal	7
	C. Estimating for all bases and clusters	9
IV.	Deviation from the limiting dynamics in the randomization approach	11
	A. The decoupling error	13
	B. The error in the local dynamics	14
V.	Reshaping Hamiltonians using Trotterization	15
	A. Decoupling the dynamics using Trotterization	15
	B. Isolating the diagonal Hamiltonian using Trotterization	16
VI.	Deviation from the limiting dynamics in Trotterization	18
VII.	Lower bound for learning Hamiltonian from dynamics	19
	A. Model of quantum experiments	19
	B. Learning task and lower bound	20
	C. Proof of Theorem 26	21
	1. Reduction	21
	2. TV upper bound for a single experiment	21
	3. TV upper bound for many experiments	22
	4. Lower bound from TV upper bound	24
	References	24

I. PRELIMINARIES

We begin with definitions used throughout the work as well as a basic lemma that follows immediately from the chromatic number of a graph.

A. Notations

Throughout this work, we will write Q^P to denote the set of all mappings from P to Q for finite sets P and Q. We also denote $[N] = 1, 2, \dots, N$. For the product of a sequence of operators O_1, O_2, \dots, O_L , we write

$$\prod_{1 \le l \le L}^{\leftarrow} O_l = O_L \cdots O_2 O_1, \quad \prod_{1 \le l \le L}^{\rightarrow} O_l = O_1 O_2 \cdots O_L. \tag{1}$$

We generally omit the arrows when taking a product of commuting operators. We use [A, B] = AB - BA to denote the commutator between A and B, and we also write $\operatorname{ad}_A(B) = [A, B]$. Throughout this work when we say that an operator is diagonal relative to a basis, what we mean is:

Definition 1 (Diagonal operator). Let $B = \{|v_l\rangle\}$ be a basis of a Hilbert space. We say an operator O is diagonal relative to B if B is an eigenbasis of O.

For a subsystem A of the N-qubit system we consider, we use tr_A to denote the partial trace after tracing out A. By extension, we use $\operatorname{tr}_{[N]\setminus A}$ to denote the partial trace after tracing out all qubits not contained in A. We consider I to be the identity matrix, X to be the Pauli-X matrix, Y to be the Pauli-Y matrix, and Z to be the Pauli-Z matrix. We consider an N-qubit Pauli operator P to be an element in the set of N-qubit observables $\{I, X, Y, Z\}^{\otimes N}$. We also use subscript to denote which qubit the Pauli operator acts on. For example, we use X_{α} to denote the Pauli-X operator acting on qubit α , and γ_{α} , $\gamma \in \{I, X, Y, Z\}$, to denote all Pauli operators acting on this qubit.

B. Hamiltonians

We begin with a brief overview of the terminology for interacting many-body Hamiltonians.

- Local Hamiltonians are Hamiltonians $H = \sum_{i} h_{j}$, where each interaction term h_{j} acts only on $\mathcal{O}(1)$ qubits.
- Geometrically-local Hamiltonians are local Hamiltonians that only involve geometrically-local interactions, i.e., h_j only acts on nearby qubits under some geometric distance. The notion of distance comes from an underlying geometry, such as one-dimensional chains, two-dimensional square lattices, three-dimensional cubic lattices, hexagonal lattices, Kagome lattices, etc.
- Low-intersection Hamiltonians, also known as bounded-degree local Hamiltonians, are local Hamiltonians where each qubit only has constantly many interaction terms acting on it. It is not hard to show that a geometrically local Hamiltonian is a special case of a low-intersection Hamiltonian.

By expanding any Hermitian operator h_j in the Pauli basis $\{I, X, Y, Z\}^{\otimes n}$, we can establish the following definition.

Definition 2 (Low-intersection Hamiltonian). A low-intersection Hamiltonian acting on N qubits is a Hamiltonian H that takes the following form:

$$H = \sum_{a=1}^{M} \lambda_a E_a \tag{2}$$

where each E_a is an N-qubit Pauli operator acting non-trivially on at most $k = \mathcal{O}(1)$ qubits, and for each a, E_a overlaps with $\mathfrak{d} = \mathcal{O}(1)$ of E_b 's.

Following Ref. [1], we assume that E_a 's are known a priori, and the goal is to estimate λ_a for each a. Also, as a consequence of $k, \mathfrak{d} = \mathcal{O}(1)$, we have $M = \mathcal{O}(N)$. Below we introduce a set \mathcal{V} to describe how the qubits interact with each other.

Definition 3 (Interacting cluster). For each a, let $\mathrm{Supp}(E_a)$ be the support of E_a , i.e., the collection of qubits on which E_a acts nontrivially. From the set $\{\mathrm{Supp}(E_a)\}$, we remove all $\mathrm{Supp}(E_a)$ such that $\mathrm{Supp}(E_a) \subset \mathrm{Supp}(E_b)$ for some $b \in [M]$. The remaining $\mathrm{Supp}(E_a)$'s form the set V. Each element of V we call an interacting cluster.

From the above construction it is clear that $|\mathcal{V}| \leq M$. We then define the cluster interaction graph as follows.

Definition 4 (Cluster interaction graph). The cluster interaction $\mathcal{G} = (\mathcal{V}, \mathcal{E})$ has interacting clusters (from \mathcal{V} in Definition 3) as its vertices. The set of edges \mathcal{E} is defined as follows: for each pair of interacting clusters C and C' ($C \neq C'$) in \mathcal{V} , (C, C') $\in \mathcal{E}$ if $C \cap C' \neq \emptyset$ or if there exists $C'' \in \mathcal{V}$ such that $C \cap C'' \neq \emptyset$ and $C' \cap C'' \neq \emptyset$.

From the definition of the low-intersection Hamiltonian, the degree of \mathcal{G} , $\deg(\mathcal{G})$, is upper bounded by a constant that is independent of the system size N. More precisely, $\deg(\mathcal{G}) \leq \mathfrak{d}^2$ where \mathfrak{d} is defined in Definition 2.

For parallel estimation of different interacting clusters, we need to color the graph \mathcal{G} so that adjacent vertices have different colors. The number of colors χ needed, which is the chromatic number of the graph, satisfies $\chi \leq \deg(\mathcal{G}) + 1 = \mathcal{O}(1)$. Therefore we have the following lemma

Lemma 5 (Coloring of the cluster interaction graph). V can be divided into disjoint union

$$\mathcal{V} = \bigsqcup_{c=1}^{\chi} \mathcal{V}_c,\tag{3}$$

where no two adjacent vertices are in the same V_c . In other words, for any C and C' in V_c , $C \cap C' = \emptyset$, and for any $C'' \in V$, either $C \cap C'' = \emptyset$ or $C' \cap C'' = \emptyset$. Moreover $\chi = \mathcal{O}(1)$.

II. RESHAPING HAMILTONIANS USING RANDOMIZATION

Below we describe how to reshape the unknown N-qubit Hamiltonian H into a new Hamiltonian with a simpler form based on a randomized Hamiltonian simulation algorithm known as qDRIFT [2]. Given a probability distribution \mathcal{D} over N-qubit Pauli operators $\{I, X, Y, Z\}^{\otimes N}$, we consider the new Hamiltonian after reshaping to be

$$\widetilde{H}(\mathcal{D}) \triangleq \underset{P \sim \mathcal{D}}{\mathbb{E}}[PHP].$$
 (4)

The qDRIFT algorithm can approximate (as a quantum channel) dynamics under $\widetilde{H}(\mathcal{D})$ by dynamics under H as follows,

$$e^{-it\tilde{H}(\mathcal{D})} \approx e^{-i\tau P_{k_r}HP_{k_r}} \dots e^{-i\tau P_{k_1}HP_{k_1}} = P_{k_r}e^{-i\tau H}P_{k_r} \dots P_{k_1}e^{-i\tau H}P_{k_1},$$
 (5)

where r is an integer that determines the approximation error (larger r implies smaller error), $\tau \triangleq t/r$, and P_{k_1}, \ldots, P_{k_r} are independent random Pauli operators sampled from \mathcal{D} . In the original paper [2] on qDRIFT, it was shown that the approximation holds when one considers the expectation of the unitary (treated as a quantum channel) over the random Pauli operators P_{k_1}, \ldots, P_{k_r} . In a subsequent work [3], it was shown that the approximation holds even with a single realization of P_{k_1}, \ldots, P_{k_r} with high probability.

By choosing different distribution \mathcal{D} , we can reshape the unknown Hamiltonian H into new Hamiltonians with a much simplified form. In particular, the reshaping technique is useful for: (1) decoupling the N-qubit system into many few-qubit noninteracting patches, and (2) isolating the diagonal Hamiltonian in each of the few-qubit patches.

A. Decoupling into noninteracting patches

Recall that for each color $c \in [\chi]$, \mathcal{V}_c is a set of interacting clusters (i.e., few-qubit patches). For each color $c \in [\chi]$, we define a distribution \mathcal{D}_c over $P \in \{I, X, Y, Z\}^{\otimes N}$ as follows. For each qubit $\alpha \in [N]$,

- If qubit α is in one of the interacting clusters in \mathcal{V}_c , we consider $P_{\alpha} = I$.
- If qubit α is not in any of the interacting clusters in \mathcal{V}_c , we sample $P_{\alpha} \in \{I, X, Y, Z\}$ uniformly.

Then we let $P = \prod_{\alpha} P_{\alpha}$. We establish the following lemma.

Lemma 6 (Decoupling into noninteracting patches). Defining \mathcal{D}_c as above, we have

$$\widetilde{H}(\mathcal{D}_c) = \underset{P \sim \mathcal{D}_c}{\mathbb{E}}[PHP] = \sum_{C \in \mathcal{V}_c} H_C, \tag{6}$$

where $H_C \triangleq \sum_{a: \text{Supp}(E_a) \subset C} \lambda_a E_a$ is the sum of all terms in H that are supported on C.

Proof. Recall that $H = \sum_a \lambda_a E_a$. For each a, we consider the following.

• If E_a acts non-trivially on a qubit that is not in any of the interacting clusters in V_c , then there is 1/2 probability that $P \sim \mathcal{D}_c$ commutes with E_a , so that $PE_aP = E_a$, and 1/2 probability that $P \sim \mathcal{D}_c$ anti-commutes with E_a , so that $PE_aP = -E_a$. Consequently,

$$\mathbb{E}_{P \sim \mathcal{D}_c}[PE_a P] = \frac{1}{2}(E_a - E_a) = 0. \tag{7}$$

• If E_a acts trivially on all qubits that are not in any of the interacting clusters in V_c , then $P \sim D_c$ always commutes with E_a because the supports of these two operators do not overlap. As a result, we have

$$\underset{P \sim \mathcal{D}_c}{\mathbb{E}}[PE_a P] = E_a. \tag{8}$$

Therefore $\widetilde{H}(\mathcal{D}_c) = \mathbb{E}_{P \sim \mathcal{D}}[PHP]$ contains only those terms that are supported on $\bigcup_{C \in \mathcal{V}_c} C$. Next we show that those terms are supported on only a single $C \in \mathcal{V}_c$. If E_a is supported on both $C \in \mathcal{V}_c$ and $C' \in \mathcal{V}_c$, then the support of E_a overlaps with both C and C', making them adjacent by Definition 4, which precludes them from being including in the same V_c , thus resulting in contradiction. Therefore each E_a is supported on only a single $C \in \mathcal{V}_c$.

Recall that an interacting cluster $C \in \mathcal{V}_c$ is a set of at most k qubits. Hence H_C is an N-qubit Hamiltonian that acts non-trivially on at most $k = \mathcal{O}(1)$ of qubits. For each $c \in [\chi]$, the evolution under the new Hamiltonian $H(\mathcal{D}_c)$ after reshaping is given by

$$e^{-it\widetilde{H}(\mathcal{D}_c)} = \bigotimes_{C \in \mathcal{V}_c} e^{-itH_C}, \tag{9}$$

which is decoupled into many few-qubit patches that do not interact with each other. In our algorithm we will learn all H_C 's in parallel for a given $c \in [\chi]$. Because we prepare product states in all experiments, and measure observables that are local to each $C \in \mathcal{V}_c$, we can perform all the experiments in parallel as long as we evolve for the same length of time t. To be more precise, in each experiment, we perform the evolution (in terms of the density operator)

$$\rho(0) = \bigotimes_{C \in \mathcal{V}_c} \rho_C \mapsto e^{-i\tilde{H}(\mathcal{D}_c)t} \rho(0) e^{i\tilde{H}(\mathcal{D}_c)t} = \bigotimes_{C \in \mathcal{V}_c} e^{-iH_C t} \rho_C e^{iH_C t}, \tag{10}$$

where $\rho(0)$ is the initial state, and ρ_C is the initial state for each $C \in \mathcal{V}_c$. The qubits not contained in $\bigcup_{C \in \mathcal{V}_c} C$ are neglected because they are decoupled from the dynamics. We then measure observables O_C (supported on C) for each C individually. The quantities we extract from the experiments are

$$\operatorname{tr}[O_C e^{-iH_C t} \rho_C e^{iH_C t}] = \operatorname{tr}[(O_C \otimes I) e^{-i\widetilde{H}(\mathcal{D}_c)t} \rho(0) e^{-i\widetilde{H}(\mathcal{D}_c)t}], \tag{11}$$

where the identity operator I acts on $[N] \setminus C$. We do not need to rerun the experiment for each C because O_C 's commute with each other. Therefore, from now on we focus on a single C and discuss how to learn H_C .

Isolating the diagonal Hamiltonian

Recall from Section IA that any $\gamma \in \{I, X, Y, Z\}^C$ is a function mapping from a subset of qubits $C \subseteq [N]$ to a Pauli operator $\{I, X, Y, Z\}$. Using this notation, we can write down the Hamiltonian H_C in the Pauli basis as follows,

$$H_C = \sum_{\gamma \in \{I, X, Y, Z\}^C} \lambda_{\gamma} \prod_{\alpha \in C} \gamma(\alpha)_{\alpha}, \tag{12}$$

where $\gamma(\alpha)_{\alpha}$ is the Pauli operator $\gamma(\alpha)$ acting on qubit α . Hence, learning H_C is equivalent to learning λ_{γ} 's. Each λ_{γ} corresponds to λ_a in (2) for some $a \in [M]$. More specifically, $\lambda_{\gamma} = \lambda_a$ for $a \in [M]$ with $E_a = \prod_{\alpha \in C} \gamma(\alpha)_{\alpha}$ (if there does not exist such an a then $\lambda_{\gamma} = 0$). In order to learn H_C , we again utilize the reshaping technique. We reshape the Hamiltonian H_C into a easier-to-learn form using the following distributions. Given $\gamma \in \{X, Y, Z\}^C$. We define the distribution $\mathcal{D}_{C,\gamma}$ over N-qubit Pauli operator Q as follows. For each qubit $i \in [N]$,

- If qubit α is in C, we consider $Q_{\alpha} = I$ or $\gamma(\alpha)$ with equal probability.
- If qubit α is not in C, we consider $Q_{\alpha} = I$.

Then we let $Q = \prod_{\alpha} Q_{\alpha}$. We can establish the following lemma showing the new Hamiltonian $\widetilde{H_C}(\mathcal{D}_{C,\gamma})$ after reshaping.

Lemma 7 (Isolating the diagonal Hamiltonian). Using the definition of $\mathcal{D}_{C,\gamma}$, we have

$$\widetilde{H_C}(\mathcal{D}_{C,\gamma}) = \underset{Q \sim \mathcal{D}_{C,\gamma}}{\mathbb{E}}[QH_CQ] = \sum_{b \in \{0,1\}^C} \lambda_b \prod_{\alpha \in C} (\gamma(\alpha)_\alpha)^{b(\alpha)} \triangleq H_{\text{diag}}^C(\gamma), \tag{13}$$

where $\lambda_b = \lambda_{\gamma'}$ for some $\gamma' \in \{I, X, Y, Z\}^C$ given by

$$\gamma'(\alpha) = \begin{cases} I, & \text{if } b(\alpha) = 0, \\ \gamma(\alpha), & \text{if } b(\alpha) = 1. \end{cases}$$
 (14)

Proof. Each Pauli operator in H_C can be written as $P = \prod_{\alpha \in C} \gamma'(\alpha)_{\alpha}$ for some $\gamma' \in \{I, X, Y, Z\}^C$. If $\gamma(\alpha) \neq \gamma'(\alpha)$ and $\gamma'(\alpha) \neq I$ for any $\alpha \in C$, P will commute with half of the Q's and anti-commute with the other half (we can simply count for how many α 's we have $\gamma(\alpha) \neq \gamma'(\alpha)$ and $\gamma'(\alpha) \neq I$; if the number is even, P and Q commute, and if the number is odd, they anti-commute). Therefore in $\mathbb{E}_{Q \sim \mathcal{D}_{C,\gamma}}[QH_CQ]$ all these terms cancel out, and only terms that are products of $\gamma(\alpha)_{\alpha}$ for $\alpha \in C$, i.e., the diagonal terms, remain.

Let us define the Pauli eigenbases of an interacting cluster C. Using this definition, $B_C(\gamma)$ is the orthonormal eigenbasis for the diagonal Hamiltonian $H^C_{\text{diag}}(\gamma)$. This means we have acquired a very important knowledge about the new unknown Hamiltonian $H^C_{\text{diag}}(\gamma)$ after reshaping H_C : we know the eigenbasis of $H^C_{\text{diag}}(\gamma)$. In constrast, we do not know what the eigenbases for H_C are.

Definition 8 (Pauli eigenbases of an interacting cluster). For any interacting cluster C, and $\gamma \in \{X, Y, Z\}^C$, we define $B_C(\gamma)$ to be the orthonormal basis that simultaneously diagonalizes $\gamma(\alpha)_{\alpha}, \forall \alpha \in C$. We denote the set of all such bases for C by $\mathcal{B}_C = \{B_C(\gamma) : \gamma \in \{X, Y, Z\}^C\}$.

C. Combining the two reshaping procedures

We can combine the two reshaping procedures into a single one. Given a color $c \in [\chi]$, which corresponds to a set \mathcal{V}_c of many interacting clusters C, and $\gamma_C \in \{X,Y,Z\}^C$ for every interacting cluster $C \in \mathcal{V}_c$. We consider a distribution $\mathcal{D}_{c,\{\gamma_C\}_{C \in \mathcal{V}_c}}$ over N-qubit Pauli operators \bar{P} defined by Algorithm 1. In Algorithm 1, Lines 2 to 3 are for generating the P operator used in Section II A to decouple each C from the rest of the system, and Lines 4 to 6 are for generating the Q operator used in Section II B to isolate the diagonal Hamiltonian. The Pauli operator \bar{P} generated from this algorithm is therefore a product of P and Q. Consequently, from Lemmas 6 and 7, we can establish the following lemma.

Algorithm 1 Generating the random Pauli operators

```
Input: c \in [\chi], \gamma_C \in \{X, Y, Z\}^C for each C \in \mathcal{V}_c

1: for \alpha \in [N] do

2: if \alpha \notin \bigsqcup_{C \in \mathcal{V}_c} then

3: Let s_\alpha be uniformly randomly drawn from \{I, X, Y, Z\};

4: else

5: Let C be the interacting cluster containing \alpha;

6: Let s_\alpha be uniformly randomly drawn from \{I, \gamma_C(\alpha)\};

7: end if

8: end for

Output: \bar{P} = \bigotimes_{\alpha \in [N]} s_\alpha.
```

Lemma 9. Given the definition of $\mathcal{D}_{c,\{\gamma_C\}_{C\in\mathcal{V}_c}}$, we have

$$\widetilde{H}(\mathcal{D}_{c,\{\gamma_C\}_{C \in \mathcal{V}_c}}) = \underset{\bar{P} \sim \mathcal{D}_{C,\{\gamma_C\}_{C \in \mathcal{V}_c}}}{\mathbb{E}} \left[\bar{P} H \bar{P} \right] = \sum_{C \in \mathcal{V}_c} H_{\text{diag}}^C(\gamma_C), \tag{15}$$

where each $H_{\text{diag}}^{C}(\gamma_{C})$ is defined in Eq. (13).

Proof. To show this lemma, first note that

$$\mathbb{E}_{\bar{P} \sim \mathcal{D}_{C, \{\gamma_C\}_{C \in \mathcal{V}_c}}} \left[\bar{P} H \bar{P} \right] = \mathbb{E}_{\substack{Q_C \sim \mathcal{D}_{C, \gamma_C}, \\ \forall C \in \mathcal{V}_c}} \left[\left(\prod_{C \in \mathcal{V}_c} Q_C \right) \mathbb{E}_{\substack{P \sim \mathcal{D}_c}} [P H P] \left(\prod_{C \in \mathcal{V}_c} Q_C \right) \right]. \tag{16}$$

All the Pauli operators P and Q_C for all $C \in \mathcal{V}_c$ have disjoint supports. By Lemma 6 we have

$$\underset{P \sim \mathcal{D}_c}{\mathbb{E}}[PHP] = \sum_{C \in \mathcal{V}_c} H_C. \tag{17}$$

Then by Lemma 7 and Eq. (16) we have

$$\mathbb{E}_{\bar{P} \sim \mathcal{D}_{C, \{\gamma_C\}_C \in \mathcal{V}_c}} \left[\bar{P} H \bar{P} \right] = \sum_{C \in \mathcal{V}_c} \mathbb{E}_{Q_C \sim \mathcal{D}_{C, \gamma_C}} \left[Q_C H_C Q_C \right] = \sum_{C \in \mathcal{V}_c} H_{\text{diag}}^C(\gamma_C), \tag{18}$$

which establishes the lemma.

III. LEARNING THE UNKNOWN HAMILTONIAN AFTER RESHAPING

In this section we will discuss how to learn parameters (coefficients) from the new unknown Hamiltonians after reshaping. We first present how the experiments are executed in Section III A. Then we give the procedure to estimate the coefficients of terms that are diagonal in a given Pauli eigenbasis for a single cluster in Section III B. Finally, we talk about how to estimate parameters for all clusters in parallel in Section III C.

A. Executing quantum experiments

We begin by describing how the experiments are executed. Given a color $c \in [\chi]$, and a Pauli assignment $\gamma_C \in \{X,Y,Z\}^C$ for each interacting cluster $C \in \mathcal{V}_c$, we initialize the quantum system in a product state which can be prepared using single-qubit Clifford gates. We then evolve under the new unknown Hamiltonian $\widetilde{H}(\mathcal{D}_{c,\{\gamma_C\}_{C \in \mathcal{V}_c}})$ after reshaping for time t. Based on the qDRIFT algorithm, we can approximate the unitary dynamics $e^{-it\widetilde{H}(\mathcal{D}_{c,\{\gamma_C\}_{C \in \mathcal{V}_c}})}$ by

$$\bar{P}_r e^{-iH\tau} \bar{P}_r \dots \bar{P}_1 e^{-iH\tau} \bar{P}_1 = e^{-i\tau \bar{P}_r H \bar{P}_r} \dots e^{-i\tau \bar{P}_1 H \bar{P}_1}, \tag{19}$$

where r is a large integer, $\tau = t/r$, and \bar{P}_j is a random N-qubit Pauli operator sampled from distribution $\mathcal{D}_{c,\{\gamma_C\}_{C\in\mathcal{V}_c}}$ using Algorithm 1. After evolving the system, we then measure an observable O_C , supported on C, for every $C \in \mathcal{V}_c$. Because O_C 's do not overlap with each other, these measurements can be performed simulataneously. In this way we are able to estimate parameters for all clusters in \mathcal{V}_c in parallel.

Using a density matrix formulation, the experiment begins by preparing an initial state $\rho(0) = \bigotimes_{C \in \mathcal{V}_c} \rho_C \otimes \rho_{\text{res}}$, where ρ_{res} is the state of the qubits not contained in $\bigsqcup_{C \in \mathcal{V}_c} C$. After the randomized evolution, the final state before the measurements is given by

$$\rho(t) = \underset{\bar{P}_{j} \sim \mathcal{D}_{c, \{\gamma_{C}\}_{C} \in \mathcal{V}_{c}}}{\mathbb{E}} \left[\prod_{1 \leq j \leq r}^{\leftarrow} e^{-i\bar{P}_{j}H\bar{P}_{j}\tau} \rho(0) \prod_{1 \leq j \leq r}^{\rightarrow} e^{i\bar{P}_{j}H\bar{P}_{j}\tau} \right]. \tag{20}$$

In the limit of $\tau \to 0$ (equivalently $r \to \infty$), the system will evolve under $\widetilde{H}(\mathcal{D}_{c,\{\gamma_C\}_{C \in \mathcal{V}_c}}) = \sum_{C \in \mathcal{V}_c} H^C_{\text{diag}}(\gamma_C)$ as shown in Lemma 9. This means if we look at an observable supported on the interacting cluster $C \in \mathcal{V}_c$, its expectation

value will be approximately $\operatorname{tr}[O_C e^{-iH_{\operatorname{diag}}^C(\gamma_C)t}\rho_C e^{iH_{\operatorname{diag}}^C(\gamma_C)t}]$. Note that everything in this expression depends only on the cluster C.

In an actual experiment, r cannot be infinite. The theorem below tells us how small τ (or equivalently how large $r = t/\tau$) needs to be for the above procedure to achieve a given accuracy ε . The proof of this theorem is given in Section IV.

Theorem 10 (Number of required random Pauli operators). There exists $r_0 = \mathcal{O}(t^2/\varepsilon)$ such that for any $r > r_0$, any initial state $\rho(0)$, any $C \in \mathcal{V}_c$, and any O_C supported on C with $||O_C|| \le 1$, we have

$$\left| \operatorname{tr}[(O_C \otimes I)\rho(t)] - \operatorname{tr}[O_C e^{-iH_{\operatorname{diag}}^C(\gamma_C)t} \rho_C e^{iH_{\operatorname{diag}}^C(\gamma_C)t}] \right| \le \varepsilon, \tag{21}$$

where $\rho_C = \operatorname{tr}_{[N] \setminus C} \rho(0)$.

B. Estimating the diagonal

Let us focus on how to estimate the parameters for terms that are diagonal in a given Pauli eigenbasis $B_C(\gamma_C)$ as defined in Definition 8 for a cluster C. One advantage of having the system evolve under H_{diag}^C is that we have access to its eigenstates, which we denote by $|\xi\rangle$

$$|\xi\rangle = \bigotimes_{\alpha \in C} |\psi_{\alpha}\rangle, \tag{22}$$

for $\xi \in \{0,1\}^C$, where $|\psi_{\alpha}\rangle$ is the $(-1)^{\xi(\alpha)}$ -eigenstate of $\gamma_C(\alpha)$. For example, if $\gamma_C(\alpha) = X$, then $|\psi_{\alpha}\rangle = |+\rangle$ if $\xi(\alpha) = 0$, and $|\psi_{\alpha}\rangle = |-\rangle$ if $\xi(\alpha) = 1$. Importantly, $|\xi\rangle$ can be prepared using a tensor product of single-qubit Clifford gates. For each $|\xi\rangle$, the corresponding eigenvalue can be calculated through

$$H_{\operatorname{diag}}^{C}(\gamma_{C})|\xi\rangle = \sum_{b \in \{0,1\}^{C}} \lambda_{b}(-1)^{\xi \cdot b}|\xi\rangle, \qquad (23)$$

where $\xi \cdot b = \sum_{\alpha \in C} \xi(\alpha)b(\alpha)$ is the inner product between ξ and b. The eigenvalues are therefore

$$\varepsilon_{\xi} = \sum_{b \in \{0,1\}^C} (-1)^{\xi \cdot b} \lambda_b. \tag{24}$$

The eigenvalues and the parameters are therefore related via the Hadamard transform. We can recover the parameters from the eigenvalues through

$$\lambda_b = \frac{1}{2^{|C|}} \sum_{\xi \in \{0,1\}^C} (-1)^{\xi \cdot b} \varepsilon_{\xi}. \tag{25}$$

From the above discussion we can see that the parameters λ_b can be estimated from the eigenvalues ε_{ξ} . Rather than estimating ε_{ξ} directly, which is impossible because of the presence of a global gauge, we will estimate $\varepsilon_{\xi} - \varepsilon_{\xi'}$ for pairs of ξ and ξ' . Moreover from (25) we can see that, with the exception of the global phase λ_{0^C} (we denote by 0^C that maps all elements of C to 0), all other λ_b 's depend only on the differences between ε_{ξ} 's. To this end we need to prepare a superposition of $|\xi\rangle$ and $|\xi'\rangle$. We note that when the Hamming distance between ξ and ξ' is 1, then this is easy to do, because $(|\xi\rangle + |\xi'\rangle)/\sqrt{2}$ is still a product state, and each of its tensor product component can be prepared using a single Clifford gate. We denote the unitary preparing this state by

$$U_{\xi\xi'}|0^{|C|}\rangle = \frac{1}{\sqrt{2}}(|\xi\rangle + |\xi'\rangle). \tag{26}$$

This unitary is a tensor product of single-qubit Clifford gates. Similarly we can construct a unitary in the form of single-qubit Clifford gates that satisfy

$$V_{\xi\xi'}|0^{|C|}\rangle = \frac{1}{\sqrt{2}}(|\xi\rangle + i|\xi'\rangle). \tag{27}$$

This can be done by replacing the Hadamard gate in $U_{\xi\xi'}$ with SH where S is the phase gate.

Now we run experiments as follows: starting from $|0^{|C|}\rangle$, we apply $U_{\xi\xi'}$, and then evolve with $e^{-iH_{\text{diag}}^C(\gamma_C)t}$ (which is approximately obtained by randomly applying P_j and Q_j as discussed above). Then we apply $U_{\xi\xi'}^{\dagger}$, and measure all the k qubits. The probability of all qubits being returned to the 0 state is

$$|\langle 0^{|C|}|U_{\xi\xi'}^{\dagger}e^{-iH_{\operatorname{diag}}^{C}(\gamma_{C})t}U_{\xi\xi'}|0^{|C|}\rangle|^{2} = \frac{1}{2}(1+\cos((\varepsilon_{\xi}-\varepsilon_{\xi'})t)). \tag{28}$$

Similarly we can design an experiment in which the probability of returning to $|0^{|C|}\rangle$ is

$$|\langle 0^{|C|} | V_{\xi\xi'}^{\dagger} e^{-iH_{\text{diag}}^{C}(\gamma_{C})t} U_{\xi\xi'} | 0^{|C|} \rangle |^{2} = \frac{1}{2} (1 + \sin((\varepsilon_{\xi} - \varepsilon_{\xi'})t)). \tag{29}$$

We let $\tau' = \pi/2^{|C|+2}$ so that $\tau'|\varepsilon_{\xi} - \varepsilon_{\xi'}| \le \pi/2$ (we know from (24) that $|\varepsilon| \le 2^{|C|}$). Then let $t = \ell \tau'$ for positive integer ℓ , the two probabilities in (28) and (29) become

$$p_0(\ell) = \frac{1}{2} (1 + \cos(\ell \tau'(\varepsilon_{\xi} - \varepsilon_{\xi'}))),$$

$$p_+(\ell) = \frac{1}{2} (1 + \sin(\ell \tau'(\varepsilon_{\xi} - \varepsilon_{\xi'}))),$$
(30)

corresponding to the probabilities in [4, Theorem I.1]. Using the robust phase estimation technique in [4, Theorem I.1], we can then estimate $\tau'(\varepsilon_{\xi} - \varepsilon_{\xi'})$ with standard deviation $\epsilon'\tau'/3$, by running $e^{-iH_{\text{diag}}^C(\gamma_C)\tau'} \mathcal{O}(\epsilon'^{-1}\tau'^{-1})$ times. Therefore the total evolution time with H is $\mathcal{O}(\epsilon'^{-1}\tau'^{-1}) \times \tau' = \mathcal{O}(\epsilon'^{-1})$. The number of experiments scale like $\mathcal{O}(\text{polylog}(\epsilon'^{-1}\tau'^{-1})) = \mathcal{O}(\text{poly}(|C| + \log(\epsilon'^{-1}))) \leq \mathcal{O}(\text{poly}(k + \log(\epsilon'^{-1})))$. Here we use the fact that $|C| \leq k$.

With this we can estimate $\varepsilon_{\xi} - \varepsilon_{\xi'}$ with standard deviation $\epsilon'/3$. Our ultimate goal is to ensure that the estimate has low error with high probability. Therefore we can repeat the experiment $\mathcal{O}(\log(\vartheta^{-1}))$ times and take the median to ensure that the error is below ϵ' with probability at least $1 - \vartheta$. In the procedure above, in order to estimate $\varepsilon_{\xi} - \varepsilon_{\xi'}$ to precision ϵ' with probability at least $1 - \vartheta$, we need a total evolution time of

$$\mathcal{O}(\epsilon'^{-1}\log(\vartheta^{-1})),\tag{31}$$

and the number of experiments required is

$$\mathcal{O}(\text{poly}(k + \log(\epsilon'^{-1}))\log(\vartheta^{-1})). \tag{32}$$

The above procedure only gets us the differences $\varepsilon_{\xi} - \varepsilon_{\xi'}$ for ξ and ξ' that differ by one bit. Next we will discuss how to estimate each ε_{ξ} . Because the global phase is undetectable we can assume $\varepsilon_{0^C} = 0$ (here ε_{0^C} is the eigenvalue corresponding to the mapping that maps all elements of C to 0). We can then estimate each ε_{ξ} by the Hamming weight of ξ . Starting with w = 1, once we have $\varepsilon_{\xi'}$ for all ξ' with Hamming weight w - 1, we can estimate all ε_{ξ} with Hamming weight w, by estimating $\varepsilon_{\xi} - \varepsilon_{\xi'}$ for some ξ' that differs from ξ by one bit and has Hamming weight w - 1. This allows us to estimate all ε_{ξ} , each of which through

$$\varepsilon_{\xi} = \sum_{l=0}^{w-1} (\varepsilon_{\xi_{l+1}} - \varepsilon_{\xi_l}), \tag{33}$$

where $\xi_w = \xi$, $\xi_0 = 0^C$ (which means ξ_0 maps all elements of C to 0), ξ_l has Hamming weight l, and ξ_{l+1} and ξ_l differ by only one bit. Because the summand on the right-hand side has at most $|C| \le k$ terms, we only need to estimate each $\varepsilon_{\xi_{l+1}} - \varepsilon_{\xi_l}$ to precision $\epsilon' = \epsilon/k$ to ensure that the final error is at most ϵ .

This procedure can be seen as traversing a shortest path tree: if we define a graph with all $\xi \in \{0,1\}^C$ as vertices, and link ξ and ξ' if their Hamming distance is 1, we will have a |C|-hypercube. Then we can define the shortest path tree as follows.

Definition 11 (Shortest path tree). The shortest path tree $\mathcal{T}^{C}_{SPT} = (\{0,1\}^{C}, \mathcal{E}^{C}_{SPT})$ is a subgraph of the |C|-hypercube, with root 0^{C} , and \mathcal{E}^{C}_{SPT} is the set of edges. \mathcal{T}^{C}_{SPT} satisfies that the path from the root to each vertex in the tree has the shortest distance in the |C|-hypercube.

For each $(\xi, \xi') \in \mathcal{E}_{SPT}^C$, we estimate $\varepsilon_{\xi} - \varepsilon_{\xi'}$, and with this we can obtain the value of any ε_{ξ} by traversing the path leading from 0^C to ξ in \mathcal{T}_{SPT}^C .

There are in total $2^{|C|} - 1$ pairs of ξ and ξ' such that we need to estimate $\varepsilon_{\xi} - \varepsilon_{\xi'}$, because a tree with $2^{|C|}$ nodes has $2^{|C|} - 1$ edges. In order to ensure that each estimate of ε_{ξ} has confidence level $1 - \delta$, each $\varepsilon_{\xi} - \varepsilon_{\xi'}$ needs a confidence

level of $1 - \delta/k$ by union bound. Therefore, substituting $\epsilon' = \epsilon/k$ and $\vartheta = \delta/k$ into (31), for each $\varepsilon_{\xi} - \varepsilon_{\xi'}$ the total evolution time we need is

$$\mathcal{O}(k\epsilon^{-1}\log(k\delta^{-1})),\tag{34}$$

and the number of experiments needed is, by substituting into (32),

$$\mathcal{O}(\text{poly}(k + \log(k\epsilon^{-1}))\log(k\delta^{-1})).$$
 (35)

Once all ε_{ξ} are estimated with precision ϵ , we can get all λ_b in (13) with precision ϵ through (25).

C. Estimating for all bases and clusters

In Section IIIB we have focused on a single interacting cluster and a fixed Pauli eigenbasis. This procedure needs to be repeated for all interacting clusters C, the number of which is upper bounded by M, and for all $3^{|C|}$ possible choices of basis (there is a lot of double counting involved, for which further optimization may be possible), in order to cover the parameters of all terms involved in (2). Note that in Sections II A and II C we have showed that interacting clusters within the same V_c (having the same color in the coloring of the cluster interaction graph \mathcal{G}) can be estimated in parallel. Therefore we only need an overhead of $\chi = \mathcal{O}(\mathfrak{d}^2)$ (the chromatic number in Lemma 5) rather than M to get all interacting clusters.

Algorithm 2 Learning the Hamiltonian

```
Input: Low-intersection Hamiltonian H (Definition 2)
 1: Generate the cluster interaction graph \mathcal{G} = (\mathcal{V}, \mathcal{E}) (Definition 4);
 2: Color the cluster interaction graph: \mathcal{V} = \bigsqcup_{c \in [\chi]} \mathcal{V}_c (Lemma 5);
 3: for C \in \mathcal{V} do
         Generate \mathcal{T}_{SPT}^C = (\mathcal{V}_{SPT}^C, \mathcal{E}_{SPT}^C), the shortest path tree of the |C|-hypercube (Definition 11);
 4:
 5: end for
 6: for c \in [\chi] do
        Let \mathcal{S}_C = \{(\gamma, \xi, \xi') : \gamma \in \{X, Y, Z\}^C, (\xi, \xi') \in \mathcal{E}_{\mathrm{SPT}}^C\} for each C \in \mathcal{V}_c; while \sum_{C \in \mathcal{V}_c} |\mathcal{S}_C| > 0 do for C \in \mathcal{V}_c do
 7:
 8:
 9:
                if S_C \neq \emptyset then
10:
                    Choose (\gamma_C, \xi_C, \xi_C') \in \mathcal{S}_C;
Discard (\gamma_C, \xi_C, \xi_C') from \mathcal{S}_C;
11:
12:
13:
                    Randomly draw \gamma_C from \{X,Y,Z\}^C; {This step is merely for notation consistency; we can let C remain idle
14:
                    when S_C = \emptyset.
                end if
15:
             end for
16:
             Generate random Pauli operators \{\bar{P}_j\} using Algorithm 1 (with c and \{\gamma_C\} as input);
17:
            Use robust phase estimation [4] to estimate \varepsilon_{\xi_C} - \varepsilon_{\xi'_C} for all C \in \mathcal{V}_c simultaneously, by letting the system evolve under
18:
            H and inserting the Pauli operators \{\bar{P}_j\} (Section III B, insertion of random Pauli operators described in Section II C);
         end while
19:
         for C \in \mathcal{V}_c, \gamma_C \in \{X, Y, Z\}^C do
20:
            Use \{\varepsilon_{\xi_C} - \varepsilon_{\xi_C'} : (\xi_C, \xi_C') \in \mathcal{E}_{SPT}^C\} generated above to generate estimate \hat{\lambda}_a for parameter \lambda_a of each term supported
21:
             on C and diagonal in the Pauli eigenbasis B_C(\gamma_C) (Sections IIIB and IIIC, for the Pauli eigenbasis see Definition 8);
         end for
22:
23: end for
Output: Estimate \hat{\lambda}_a of \lambda_a for each a \in [M].
```

We summarize our procedure in Algorithm 2. From (34) and (35), we can get the total evolution time and number of experiments needed to learn all the parameters to within error ϵ , with a confidence level of $1 - \delta$ for each estimate: they are respectively

$$3^{k}\chi \times (2^{k} - 1) \times \mathcal{O}(k\epsilon^{-1}\log(k\delta^{-1})) = \mathcal{O}(k6^{k}\mathfrak{d}^{2}\epsilon^{-1}\log(k\delta^{-1})),\tag{36}$$

and

$$3^{k}\chi \times (2^{k} - 1) \times \mathcal{O}(\operatorname{poly}(k + \log(k\epsilon^{-1})) \log(k\delta^{-1})) = \mathcal{O}(6^{k}\mathfrak{d}^{2}\operatorname{poly}(k + \log(k\epsilon^{-1})) \log(k\delta^{-1})). \tag{37}$$

When $k = \mathcal{O}(1)$ and $\mathfrak{d} = \mathcal{O}(1)$, they become $\mathcal{O}(\epsilon^{-1}(\log(\delta^{-1})))$ and $\mathcal{O}(\text{polylog}(\epsilon^{-1})\log(\delta^{-1}))$ respectively.

In the above analysis we only considered the $\tau \to 0$ limit, i.e., we apply random Pauli operators infinitely frequently. This is impossible in reality. Fortunately, the robust phase estimation algorithm we use is robust to error below a constant threshold. More precisely, in (28) and (29), we can tolerate an error up to $1/\sqrt{8}$ [4]. Therefore we only need to apply random Pauli operators with a finite frequency. Theorem 10 tells us what the necessary frequency is. Below we summarize the cost of our algorithm.

Theorem 12. Assume the following: for any t > 0, $c \in [\chi]$, $\{\gamma_C\}_{C \in \mathcal{V}_c}$ (with χ and \mathcal{V}_c defined in Lemma 5), we can start from initial state $\rho(0) = \bigotimes_{C \in \mathcal{V}_c} \rho_C \otimes \rho_{\text{res}}$ (each ρ_C is a density matrix for C, and ρ_{res} is the density matrix for the qubits not contained in $\bigsqcup_{C \in \mathcal{V}_c} C$) and apply random Pauli operators so that at time t the quantum system, evolving under Hamiltonian (2), is in the state $\rho(t)$ satisfying

$$\left| \operatorname{tr}[O_C e^{-iH_{\operatorname{eff}}^C(\gamma_C)t} \rho_C e^{iH_{\operatorname{eff}}^C(\gamma_C)t}] - \operatorname{tr}[(O_C \otimes I)\rho(t)] \right| \le \frac{1}{\sqrt{8}},\tag{38}$$

where $H_{\text{eff}}^C(\gamma_C)$ is as defined in (13) (for $\gamma = \gamma_C$), and O_C is any Hermitian operator supported on C with $||O_C|| \le 1$. Under this assumption, we can generate estimates $\{\hat{\lambda}_a\}$ for parameters $\{\lambda_a\}$ in (2), such that

$$\Pr[|\hat{\lambda}_a - \lambda_a| > \epsilon] < \delta \tag{39}$$

for all $a \in [M]$ with the following cost:

- 1. $\mathcal{O}(k6^k \mathfrak{d}^2 \epsilon^{-1} \log(k\delta^{-1}))$ total evolution time;
- 2. $\mathcal{O}(6^k \mathfrak{d}^2 \operatorname{poly}(k + \log(k\epsilon^{-1})) \log(k\delta^{-1}))$ number of experiments.

By Theorem 10, the condition (38) in the above theorem can be satisfied by choosing $r = \mathcal{O}(t^2)$. Therefore we arrive at our main result:

Theorem 13 (Learning many-body Hamiltonian by reshaping with randomization). Assume that H is a low-intersection Hamiltonian defined in Definition 2. Then using Algorithm 2, we can generate estimates $\{\hat{\lambda}_a\}$ for parameters $\{\lambda_a\}$ in (2), such that

$$\Pr[|\hat{\lambda}_a - \lambda_a| > \epsilon] < \delta \tag{40}$$

for all $a \in [M]$ with the following cost:

- 1. $\mathcal{O}(\epsilon^{-1}\log(\delta^{-1}))$ total evolution time:
- 2. $\mathcal{O}(\text{polylog}(\epsilon^{-1})\log(\delta^{-1}))$ number of experiments:
- 3. $\mathcal{O}(N\epsilon^{-2}\operatorname{polylog}(\epsilon^{-1})\log(\delta^{-1}))$ single-qubit Clifford qates;

Moreover, this algorithm is robust against SPAM error.

Note that in this theorem we assume $\mathfrak{d} = \mathcal{O}(1)$ and $k = \mathcal{O}(1)$, and therefore do not consider the dependence on these two parameters.

Proof. The total evolution time and the number of experiments are direct consequences of Theorem 12. Therefore we only need to focus on how many single-qubit Clifford gates are needed. For each experiment, we need $\mathcal{O}(N)$ such gates in $U_{\xi\xi'}$ (defined in (26)) to prepare the initial state and in $V_{\xi\xi'}$ (defined in (27)) to perform measurements. These two tasks require $\mathcal{O}(N\text{polylog}(\epsilon^{-1})\log(\delta^{-1}))$ single-qubit Clifford gates as a result. For each experiment, if the time evolution goes from 0 to t, then $r = \mathcal{O}(t^2)$, meaning that we need $\mathcal{O}(Nt^2)$ single-qubit Clifford gates to implement the random Pauli operators. $t = \mathcal{O}(\epsilon^{-1})$ for all experiments due to [4], and therefore the total number of single-qubit Clifford gates is $\mathcal{O}(N\epsilon^{-2})$ multiplied by the number of experiments $\mathcal{O}(\text{polylog}(\epsilon^{-1})\log(\delta^{-1}))$, yielding the scaling stated in the theorem.

To see why the algorithm is robust against SPAM error, note that the probabilities of the output distribution can differ from those in (28) and (29) by as much as $1/\sqrt{8}$, and the robust phase estimation algorithm in [4] will still work. As a result our algorithm can tolerate SPAM error below the threshold $1/\sqrt{8}$.

IV. DEVIATION FROM THE LIMITING DYNAMICS IN THE RANDOMIZATION APPROACH

In this section we will prove Theorem 10. In fact, we will prove a stronger result, as stated in the following theorem:

Theorem 14. We assume that H is a low-intersection Hamiltonian as defined in Definition 2. We assume random Pauli operators \bar{P}_l , $1 \le l \le r$, are generated independently and are identically distributed as \bar{P} , which satisfies

$$\mathbb{E}[\bar{P}H\bar{P}] = H_{\text{eff}}^C + H_{\text{env}},\tag{41}$$

where H_{eff}^C is supported on a subsystem C ($|C| = \mathcal{O}(1)$) and H_{env} is supported on the rest of the system. Then

$$\left\| \mathbb{E} \left[\prod_{1 \le l \le r}^{\to} (\bar{P}_l e^{iH\tau} \bar{P}_l) (O_C \otimes I) \prod_{1 \le l \le r}^{\leftarrow} (\bar{P}_l e^{-iH\tau} \bar{P}_l) \right] - e^{iH_{\text{eff}}^C t} O_C e^{-iH_{\text{eff}}^C t} \otimes I \right\| = \mathcal{O}(t^2/r), \tag{42}$$

for any O_C supported on C satisfying $||O_C|| \le 1$. In particular, the constant in $\mathcal{O}(t^2/r)$ does not depend on the system size N or the number of terms M.

We will postpone proving this theorem to later. As can be seen from (42), this theorem concerns the evolution of a local observable O_C in the Heisenberg picture. At time t, with the system evolving under H and random Pauli operators inserted, O_C becomes

$$\mathbb{E}\left[\prod_{1\leq l\leq r}^{\rightarrow} (\bar{P}_l e^{iH\tau} \bar{P}_l)(O_C \otimes I) \prod_{1\leq l\leq r}^{\leftarrow} (\bar{P}_l e^{-iH\tau} \bar{P}_l)\right]$$
(43)

in the Heisenberg picture and in the $\tau \to 0$ limit it should converge to

$$e^{iH_{\rm eff}^C t} O_C e^{-iH_{\rm eff}^C t} \otimes I.$$
 (44)

What the above theorem says is the following: when then random Pauli operators \bar{P}_l 's are applied sufficiently frequently, the evolution of O_C is entirely determined by the local effective Hamiltonian H_{eff}^C up to a small error. The local effective Hamiltonian H_{eff}^C , in the context of our algorithm, is $H_{\text{diag}}^C(\gamma)$ defined in (13). If we turn our attention to the observable expectation value, then the above theorem directly enables us to bound the error in observable expectation value, through the following corollary:

Corollary 15. Under the same assumption as Theorem 14, if the system is initially in a state $\rho(0)$, and at time t evolves to

$$\rho(t) = \mathbb{E}\left[\prod_{1 \le l \le r}^{\leftarrow} e^{-i\bar{P}_j H \bar{P}_j \tau} \rho(0) \prod_{1 \le l \le r}^{\rightarrow} e^{i\bar{P}_j H \bar{P}_j \tau}\right],\tag{45}$$

then

$$\left| \operatorname{tr}[(O_C \otimes I)\rho(t)] - \operatorname{tr}[O_C e^{-iH_{\text{eff}}^C t} \rho_C e^{iH_{\text{eff}}^C t}] \right| = \mathcal{O}(t^2/r), \tag{46}$$

where $\rho_C = \operatorname{tr}_{env} \rho(0)$ (tr_{env} denotes the partial trace after tracing out the system outside C), and O_C is supported on C with $||O_C|| \le 1$.

Before we prove this corollary let us first introduce some notations. The actual dynamics of the operator O_C supported on C at time $t_u = u\tau$ for $1 \le u \le r$, when the system is evolving under H with random Pauli operators inserted as described in Section II C, is described by

$$O_C^{(u)} = \mathbb{E}\left[\prod_{1 \le l \le u}^{\rightarrow} (\bar{P}_l e^{iH\tau} \bar{P}_l)(O_C \otimes I) \prod_{1 \le l \le u}^{\leftarrow} (\bar{P}_l e^{-iH\tau} \bar{P}_l)\right],\tag{47}$$

where $O_C^{(r)}$ is the operator we get at time t, i.e., the end of the experiment. The limiting dynamics is, for $\tau \to 0$,

$$O_C(t) = e^{iH_{\text{eff}}^C t} O_C e^{-iH_{\text{eff}}^C t}.$$
(48)

Proof of Corollary 15. By Theorem 14 we have $||O_C^{(r)} - O_C(t) \otimes I|| = \mathcal{O}(t^2/r)$. The left-hand side of (46) can be written as

$$\left| \operatorname{tr}[\rho(0)O_C^{(r)}] - \operatorname{tr}[\rho(0)(O_C(t) \otimes I)] \right|$$

$$= \left| \operatorname{tr}[\rho(0)(O_C^{(r)} - O_C(t) \otimes I)] \right|$$

$$\leq \|O_C^{(r)} - O_C(t) \otimes I\|.$$
(49)

Therefore by Theorem 14 we arrive at (46).

This corollary, in turn, directly implies Theorem 10.

Proof of Theorem 10. By Lemma 9, for a fixed cluster C, we can write

$$\mathbb{E}[\bar{P}H\bar{P}] = H_{\text{diag}}^{C}(\gamma_{C}) + \sum_{C' \in \mathcal{V}_{c}, C' \neq C} H_{\text{diag}}^{C'}(\gamma_{C'}). \tag{50}$$

Here the first term on the right-hand side is supported only on C and the support of the second term on the right-hand side does not overlap with C, by virtue of the coloring in Lemma 5. Therefore the effective Hamiltonian has the form as required in (41). Thus by Corollary 15 we have

$$\left| \operatorname{tr}[(O_C \otimes I)\rho(t)] - \operatorname{tr}[O_C e^{-iH_{\operatorname{diag}}^C(\gamma_C)t} \rho_C e^{iH_{\operatorname{diag}}^C(\gamma_C)t}] \right| = \mathcal{O}(\frac{t^2}{r}). \tag{51}$$

In order to ensure that $\mathcal{O}(\frac{t^2}{r}) \leq \varepsilon$, it suffices to choose $r \geq r_0$ for some $r_0 = \mathcal{O}(t^2/\varepsilon)$.

We will then set about to prove Theorem 14.

Proof of Theorem 14. Using the notation introduced in (47) and (48), (42) can be written as

$$||O_C^{(r)} - O_C(t) \otimes I|| = \mathcal{O}\left(\frac{t^2}{r}\right). \tag{52}$$

We will prove this inequality in two steps. We define

$$\bar{O}_C^{(u)} = \left(I + i\tau \operatorname{ad}_{H_{\text{eff}}^C}\right)^u O_C, \tag{53}$$

This operator can be seen as a result of simulating the dynamics of $O_C(t)$ up to first order using Euler's method. It satisfy the following recursion relation:

$$\bar{O}_C^{(u)} = \bar{O}_C^{(u-1)} + i\tau [H_{\text{eff}}^C, \bar{O}_C^{(u-1)}]$$
(54)

with $\bar{O}_C^{(0)} = O_C$. In the first step we will show that

$$\|\bar{O}_C^{(r)} \otimes I - O_C^{(r)}\| = \mathcal{O}\left(\frac{t^2}{r}\right). \tag{55}$$

Note that the right-hand side does not depend on the system size. Because $\bar{O}_C^{(r)} \otimes I$ acts non-trivially only on the cluster C, what the above bound means is that $O_C^{(r)}$ approximately only acts non-trivially on C, despite the fact that the dynamics due to H will spread O_C to the rest of the system. This inequality will be proved as Lemma 16 in Section IV A.

In the second step, we will show that

$$||O_C(t) - \bar{O}_C^{(r)}|| = \mathcal{O}\left(\frac{t^2}{r}\right)$$

$$\tag{56}$$

Again the right-hand side does not depend on the system size. This inequality will be proved as Lemma 17 in Section IV B. For the above inequality, both $O_C(t)$ and $\bar{O}_C^{(r)}$ are local operators supported on C, and therefore it characterizes the deviation of the local dynamics from the limiting dynamics. Combining (55) and (56), we have (52) by the triangle inequality.

A. The decoupling error

In this section we will prove (55). We restate it in the following lemma

Lemma 16. Under the same assumptions as in Theorem 14, we have

$$\|\bar{O}_C^{(r)} \otimes I - O_C^{(r)}\| = \mathcal{O}\left(\frac{t^2}{r}\right),$$

where $O_C^{(r)}$ and $\bar{O}_C^{(r)}$ are defined in (47) and (53) respectively.

Proof. We define

$$M^{(u-1)} = \mathbb{E}[(\bar{P}_u e^{iH\tau} \bar{P}_u)(\bar{O}_C^{(u-1)} \otimes I)(\bar{P}_u e^{-iH\tau} \bar{P}_u)] - \bar{O}_C^{(u)} \otimes I, \tag{57}$$

and

$$R^{(u)} = M^{(u-1)} + \mathbb{E}[(\bar{P}_u e^{iH\tau} \bar{P}_u) R^{(u-1)} (\bar{P}_u e^{-iH\tau} \bar{P}_u)], \tag{58}$$

with $R^{(0)} = 0$. Then we can inductively verify that

$$O_C^{(u)} = \bar{O}_C^{(u)} \otimes I + R^{(u)}.$$
 (59)

Therefore we only need to prove that $||R^{(r)}|| = \mathcal{O}\left(\frac{t^2}{r}\right)$.

We first bound $||M^{(u-1)}||$. Using Taylor expansion, we have

$$\mathbb{E}[(\bar{P}_u e^{iH\tau} \bar{P}_u)(\bar{O}_C^{(u-1)} \otimes I)(\bar{P}_u e^{-iH\tau} \bar{P}_u)] = \sum_{i=0}^{\infty} \frac{(i\tau)^j}{j!} \mathbb{E}[\bar{P}_u \operatorname{ad}_H^j(\bar{P}_u(\bar{O}_C^{(u-1)} \otimes I)\bar{P}_u)\bar{P}_u]. \tag{60}$$

From this we want to upper bound $\|\operatorname{ad}_H^j(\bar{P}_u(\bar{O}_C^{(u-1)}\otimes I)\bar{P}_u\|$ for $j\geq 2$. We have

$$\operatorname{ad}_{H}^{j}(\bar{P}_{u}(\bar{O}_{C}^{(u-1)} \otimes I)\bar{P}_{u}) = \sum_{a_{1}, a_{2}, \cdots, a_{j}} \lambda_{a_{j}} \cdots \lambda_{a_{1}}[E_{a_{j}}, \cdots [E_{a_{1}}, \bar{P}_{u}(\bar{O}_{C}^{(u-1)} \otimes I)\bar{P}_{u}] \cdots]. \tag{61}$$

Note that for the right-hand side, most of the terms are zero. We need to figure out how many terms are non-zero. For a_1 , we note that $\bar{P}_u(\bar{O}_C^{(u-1)}\otimes I)\bar{P}_u$ is supported on C, and therefore only terms that acts non-trivially with C has non-zero contribution. Therefore we only need to consider a_1 such that $\operatorname{Supp} E_{a_1} \cap C \neq \emptyset$. For a_2 , because $\cdots [E_{a_1}, \bar{P}_u(\bar{O}_C^{(u-1)}\otimes I)\bar{P}_u]$ has support on $\operatorname{Supp} E_{a_1} \cup C$, we only need to consider a_2 such that $\operatorname{Supp} E_{a_2} \cap (\operatorname{Supp} E_{a_1} \cup C) \neq \emptyset$. From this we can conclude that the only non-zero terms are for $\vec{a} = (a_1, a_2, \cdots, a_j)$, where $\operatorname{Supp} E_{a_v} \cap (\bigcup_{v < v} \operatorname{Supp} E_{a_v} \cup C) \neq \emptyset$. We denote by A_j the set of \vec{a} satisfying the above condition, and from (61) we have

$$\operatorname{ad}_{H}^{j}(\bar{P}_{u}(\bar{O}_{C}^{(u-1)}\otimes I)\bar{P}_{u}) = \sum_{\vec{a}\in\mathcal{A}_{j}}\lambda_{a_{j}}\cdots\lambda_{a_{1}}[E_{a_{j}},\cdots[E_{a_{1}},\bar{P}_{u}(\bar{O}_{C}^{(u-1)}\otimes I)\bar{P}_{u}]\cdots].$$

Note that $|\lambda_{a_j} \cdots \lambda_{a_1}| \leq 1$, and $[E_{a_j}, \cdots [E_{a_1}, \bar{P}_u(\bar{O}_C^{(u-1)} \otimes I)\bar{P}_u] \leq 2^j \|\bar{O}_C^{(u-1)}\|$. Therefore

$$\|\operatorname{ad}_{H}^{j}(\bar{P}_{u}(\bar{O}_{C}^{(u-1)}\otimes I)\bar{P}_{u})\| \leq 2^{j}|\mathcal{A}_{j}|\|\bar{O}_{C}^{(u-1)}\|.$$
 (62)

We then count $|\mathcal{A}_j|$: for a_1 , by Definition 2, there are at most $\mathfrak{d}+1$ choices because this is the number of terms that overlap with C (which is the support of a certain term in H), and for a_2 , there are at most $2(\mathfrak{d}+1)$ choices, because the second operator can either overlap with C or the first operator. Going until a_j , we can see that we have at most $j!\mathfrak{d}^j$ choices. Consequently $|\mathcal{A}_j| \leq j!(\mathfrak{d}+1)^j$. Substituting this into (62) and further into the remainders terms in (60), we have

$$\sum_{j=2}^{\infty} \frac{\tau^{j}}{j!} \mathbb{E}[\|\bar{P}_{u} \operatorname{ad}_{H}^{j} (\bar{P}_{u} (\bar{O}_{C}^{(u-1)} \otimes I) \bar{P}_{u}) \bar{P}_{u}\|] \leq \sum_{j=2}^{\infty} (2(\mathfrak{d}+1)\tau)^{j} \|\bar{O}_{C}^{(u-1)}\| = \frac{(2(\mathfrak{d}+1)\tau)^{2}}{1 - 2(\mathfrak{d}+1)\tau} \|\bar{O}_{C}^{(u-1)}\|, \tag{63}$$

For the first two terms in (60) corresponding to j = 0, 1, we compute what they are:

$$\sum_{j=0}^{1} \frac{(i\tau)^{j}}{j!} \mathbb{E}[\bar{P}_{u} \operatorname{ad}_{H}^{j} (\bar{P}_{u} (\bar{O}_{C}^{(u-1)} \otimes I) \bar{P}_{u}) \bar{P}_{u}]$$

$$= \bar{O}_{C}^{(u-1)} \otimes I + i\tau [H_{\text{eff}}^{C}, \bar{O}_{C}^{(u-1)}] \otimes I = \bar{O}_{C}^{(u)} \otimes I,$$
(64)

where in the first equality we have used (41), and in the second equality (53). Substituting this and (63) into (60), we have

$$||M^{(u-1)}|| = ||\mathbb{E}[(\bar{P}_u e^{iH\tau} \bar{P}_u)(\bar{O}_C^{(u-1)} \otimes I)(\bar{P}_u e^{-iH\tau} \bar{P}_u)] - \bar{O}_C^{(u)} \otimes I|| \le \frac{(2(\mathfrak{d}+1)\tau)^2}{1 - 2(\mathfrak{d}+1)\tau} ||\bar{O}_C^{(u-1)}||.$$
(65)

It still remains to bound $\|\bar{O}_C^{(u-1)}\|$. To simplify our discussion, we note that for sufficiently small $\mathfrak{d}\tau$ (smaller than a constant), $\frac{(2(\mathfrak{d}+1)\tau)^2}{1-2(\mathfrak{d}+1)\tau} \leq A_1\mathfrak{d}^2\tau^2$ for some constant A_1 . From (65), we have

$$\|\bar{O}_{C}^{(u)}\| \leq \|\mathbb{E}[(\bar{P}_{u}e^{iH\tau}\bar{P}_{u})(\bar{O}_{C}^{(u-1)}\otimes I)(\bar{P}_{u}e^{-iH\tau}\bar{P}_{u})]\| + A_{1}\mathfrak{d}^{2}\tau^{2}\|\bar{O}_{C}^{(u-1)}\| \leq (1 + A_{1}\mathfrak{d}^{2}\tau^{2})\|\bar{O}_{C}^{(u-1)}\|.$$
(66)

Combining this with the assumption that $||O_C|| \leq 1$, we have

$$\|\bar{O}_C^{(u)}\| \le (1 + A_1 \mathfrak{d}^2 \tau^2)^u \le (1 + A_1 \mathfrak{d}^2 t^2 / r^2)^r \le 2,\tag{67}$$

for sufficiently small $\mathfrak{d}^2 t^2/r$. Therefore

$$||M^{(u-1)}|| = ||\mathbb{E}[(\bar{P}_u e^{iH\tau} \bar{P}_u)(\bar{O}_C^{(u-1)} \otimes I)(\bar{P}_u e^{-iH\tau} \bar{P}_u)] - \bar{O}_C^{(u)} \otimes I|| \le A_2 \mathfrak{d}^2 \tau^2, \tag{68}$$

for some constant A_2 .

With this we can now bound $R^{(u)}$. By (58), we have

$$||R^{(u)}|| \le ||M^{(u-1)}|| + ||R^{(u-1)}||. \tag{69}$$

Therefore

$$||R^{(u)}|| \le \sum_{l=1}^{u-1} ||M^{(l)}|| \le A_2 u \mathfrak{d}^2 \tau^2.$$
 (70)

In particular

$$||R^{(r)}|| \le A_2 \frac{\mathfrak{d}^2 t^2}{r},\tag{71}$$

which proves the lemma.

B. The error in the local dynamics

We now prove (56), which we restate in the following lemma:

Lemma 17. Under the same assumptions as in Theorem 14, we have

$$||O_C(t) - \bar{O}_C^{(r)}|| = \mathcal{O}\left(\frac{t^2}{r}\right),$$

where $O_C(t)$ and $\bar{O}_C^{(r)}$ are defined in (48) and (53) respectively.

Proof. Thanks to the Taylor's theorem, one has

$$\bar{O}_C^{(u)} = \bar{O}_C^{(u-1)} + i\tau [H_{\text{eff}}^C, \bar{O}_C^{(u-1)}] = e^{iH_{\text{eff}}^C \tau} \bar{O}_C^{(u-1)} e^{-iH_{\text{eff}}^C \tau} + \bar{R}^{(u-1)}, \tag{72}$$

where

$$\bar{R}^{(u-1)} = \int_0^{\tau} e^{iH_{\text{eff}}^C s} [H_{\text{eff}}^C, [H_{\text{eff}}^C, \bar{O}_C^{(u-1)}]] e^{-iH_{\text{eff}}^C s} (\tau - s) \, ds.$$
 (73)

Here by (67), one has

$$\|\bar{R}^{(u-1)}\| \le \|H_{\text{eff}}^C\|^2 \tau^2 = \|H_{\text{eff}}^C\|^2 \frac{t^2}{r^2}.$$
 (74)

Denote $t_u = u\tau$ with $u = 0, 1, \dots, r$ so that $t_r = t$. The difference between $\bar{O}_C^{(u)}$ and $O_C(t_u)$ can be written as

$$\bar{O}_C^{(u)} - O_C(t_u) = e^{iH_{\text{eff}}^C \tau} \left(\bar{O}_C^{(u-1)} - O_C(t_{u-1}) \right) e^{-iH_{\text{eff}}^C \tau} + \bar{R}^{(u-1)}.$$

Taking the norm on both sides, we have

$$\|\bar{O}_C^{(u)} - O_C(t_u)\| \le \|\bar{O}_C^{(u-1)} - O_C(t_{u-1})\| + \|\bar{R}^{(u-1)}\|.$$

It then follows from (74) and $\bar{O}_C^{(0)} - O_C(0) = 0$ that

$$\|\bar{O}_C^{(r)} - O_C(t)\| \le \sum_{u=0}^{r-1} \|\bar{R}^{(u)}\| \le \|H_{\text{eff}}^C\|^2 \frac{t^2}{r}.$$

It only remains to show that $||H_{\text{eff}}^C|| = \mathcal{O}(1)$. Recall that H_{eff}^C comes from the effective Hamiltonian $\mathbb{E}[\bar{P}H\bar{P}]$ in (41). For each term E_a in H, $\bar{P}E_a\bar{P}$ preserves its support because \bar{P} and E_a are both Pauli operators. Therefore

$$H_{\text{eff}}^C = \sum_{a:\text{Supp}E_a \subset C} \lambda_a \mathbb{E}[\bar{P}E_a\bar{P}]. \tag{75}$$

From this, and $|\lambda_a| \leq 1$, we have

$$||H_{\text{eff}}^C|| \le |\{a \in [M] : \text{Supp}E_a \subset C\}| \le 4^{|C|} \le 4^k = \mathcal{O}(1).$$
 (76)

Therefore we have proved the lemma.

V. RESHAPING HAMILTONIANS USING TROTTERIZATION

Here we consider reshaping the unknown N-qubit Hamiltonian H using the second-order Trotter formula. The main idea is the following: In the randomization approach we have constructed an effective Hamiltonian that is a sum of exponentially (in N) many terms of the form PHP, and here we will consider implementing a similar sum using the 2nd-order Trotter formula. Importantly, this time the sum involves a number of terms that is independent of N.

A. Decoupling the dynamics using Trotterization

First we define a new graph known as a qubit interaction graph.

Definition 18 (Qubit interaction graph). First denote $A_c = \bigsqcup_{C \in \mathcal{V}_c} C$, for $c \in [\chi]$ and \mathcal{V}_c defined in Lemma 5. The qubit interaction graph corresponding to color $c \in [\chi]$ is defined to be $\mathcal{G}_q^c = (\mathcal{V}_q^c, \mathcal{E}_q^c)$, where $\mathcal{V}_q^c = [N] \setminus A_c$ contains the qubits that are not contained in A_c , and for any $\alpha, \alpha' \in \mathcal{V}_q^c$ $(\alpha, \alpha') \in \mathcal{E}_q^c$ iff there exists E_a such that $\alpha, \alpha' \in \operatorname{Supp}(E_a)$ and $\operatorname{Supp}(E_a) \cap A_c \neq \emptyset$.

We also need to color this graph. The number of colors is given by the following lemma.

Lemma 19. \mathcal{G}_q^c admits a coloring with χ_q colors. Here $\chi_q \leq (\mathfrak{d}+1)(k-2)+1$ (\mathfrak{d} and k are defined in Definition 2).

Proof. We will prove that $\deg(\mathcal{G}_q^c) \leq (\mathfrak{d}+1)(k-2)$, and as a result $\chi_q \leq \deg(\mathcal{G}_q^c) + 1 \leq (\mathfrak{d}+1)(k-2) + 1$. For each qubit α , there are at most $\mathfrak{d}+1$ E_a 's such that they act non-trivially on α and on at least one qubit in \mathcal{A}_c . Each E_a acts non-trivially on at most k-1 other qubits, one of which must be in \mathcal{A}_c . Therefore there are at most $(\mathfrak{d}+1)(k-2)$ choices of α' such that $(\alpha, \alpha') \in \mathcal{E}_q^c$.

We number the colors using $[\chi_q]$. We also denote by $c_q(\alpha)$ the color of qubit α . We now show that, for each color c of the cluster interaction graph \mathcal{G} (Definition 4), we can choose Pauli operators P from a set \mathcal{P}_c (to be specified later) of size 4^{χ_q} such that

$$\frac{1}{|\mathcal{P}_c|} \sum_{P \in \mathcal{P}_c} PHP = \sum_{C \in \mathcal{V}_c} H_C + H_{\text{res}},\tag{77}$$

where H_{res} is supported on $[N] \setminus \mathcal{A}_c$. We then implement the sum on the right-hand side using the second-order Trotter formula (higher-order formulae will involve evolving backward in time and is therefore unrealistic in our setting). To be more precise, we implement

$$\prod_{1 \le \nu \le |\mathcal{P}_c|} \stackrel{}{=} e^{-iP_{\nu}HP_{\nu}\tau'} \prod_{1 \le \nu \le |\mathcal{P}_c|} \stackrel{}{=} e^{-iP_{\nu}HP_{\nu}\tau'} = \prod_{1 \le \nu \le |\mathcal{P}_c|} \stackrel{}{=} P_{\nu}e^{-iH\tau'}P_{\nu} \prod_{1 \le \nu \le |\mathcal{P}_c|} \stackrel{}{=} P_{\nu}e^{-iH\tau'}P_{\nu}, \tag{78}$$

where we order the elements in \mathcal{P}_c so that $\mathcal{P}_c = \{P_{\nu}\}$, and $\tau' = \tau/(2|\mathcal{P}_c|)$. and this will approximate $e^{-i(\sum_{C \in \mathcal{V}_c} H_C + H_{\text{res}})\tau}$ up to second order (with a remainder of order τ^3).

Now we will discuss how to choose \mathcal{P}_c . We define \mathcal{P}_c as follows:

$$\mathcal{P}_c = \Big\{ \prod_{\alpha \in [N] \setminus \mathcal{A}_c} \gamma(c_q(\alpha))_\alpha : \gamma \in \{I, X, Y, Z\}^{[\chi_q]} \Big\}, \tag{79}$$

where $A_c = \bigsqcup_{C \in \mathcal{V}_c} C$ as defined in Definition 18, and $c_q(\alpha)$ is the color of qubit α in the coloring of the qubit interaction graph. To see why (77) is true, let us look at each Pauli terms E_a of H. In the first case, if the support of E_a is contained in A_c , then $[P, E_a] = 0$ for all $P \in \mathcal{P}_c$. This is because the support of each P does not overlap with A_c by definition. Consequently $PE_aP = E_a$, and

$$\frac{1}{|\mathcal{P}_c|} \sum_{P \in \mathcal{P}_a} P E_a P = E_a. \tag{80}$$

In the second case, if the support of E_a is not contained in \mathcal{A}_c , but overlaps with \mathcal{A}_c , then we denote $\operatorname{supp}(E_a) \setminus \mathcal{A}_c = \{\alpha_1, \alpha_2, \cdots, \alpha_l\}$ where $l \leq k$. By Definition (18), in a coloring of the graph $\alpha_1, \alpha_2, \cdots, \alpha_l$ are all colored differently because they are all linked to each other. Therefore, if we uniformly randomly draw a Pauli operator from \mathcal{P}_c , each Pauli operator on $\alpha_1, \alpha_2, \cdots, \alpha_l$ will be chosen independently. From this we can see, just like previously for the randomization method, half of the Pauli operators in \mathcal{P}_c commute with E_a and the other half anti-commute. As a result

$$\frac{1}{|\mathcal{P}_c|} \sum_{P \in \mathcal{P}_c} P E_a P = 0. \tag{81}$$

In the third case, if the support of E_a is disjoint from \mathcal{A}_c , then each PE_aP also acts trivially on \mathcal{A}_c . We group these terms into the residual term H_{res} . Combining (80) and (80) we have (77).

B. Isolating the diagonal Hamiltonian using Trotterization

For each cluster $C \in \mathcal{V}_c$, we want to learn the diagonal elements of H_C with respect to a Pauli eigenbasis indexed by $\gamma_C \in \{0, x, y, z\}^C$, as defined in Definition 8.

To this end, for a set of Pauli eigenbases indexed by $\{\gamma_C\}_{C\in\mathcal{V}_c}$, we define

$$Q_c = \left\{ \prod_{C \in \mathcal{V}_c} \prod_{\alpha \in C} (\gamma_C(\alpha)_\alpha)^{b_{\zeta_C(\alpha)}} : b_1, b_2, \cdots, b_k \in \{0, 1\} \right\}, \tag{82}$$

where $\zeta_C: C \to [|C|]$ is an arbitrary fixed ordering of C. Then we will have

$$\frac{1}{|\mathcal{Q}_c||\mathcal{P}_c|} \sum_{Q \in \mathcal{Q}_c} \sum_{P \in \mathcal{P}_c} QPHPQ = \sum_{C \in \mathcal{V}_c} H_{\text{diag}}^C(\gamma_C) + H_{\text{res}}, \tag{83}$$

where

$$H_{\text{diag}}^{C}(\gamma_{C}) = \frac{1}{|\mathcal{Q}_{c}|} \sum_{Q \in \mathcal{Q}_{c}} Q H_{C} Q. \tag{84}$$

is the diagonal of the Hamiltonian H_C with respect to the Pauli eigenbasis indexed by γ_C . It is the same Hamiltonian as given in (13). Therefore, to extract the diagonal Hamiltonian, we can implement

$$\mathcal{U}(\tau) = \prod_{1 \leq \nu \leq |\mathcal{R}_{c}|} \stackrel{e^{-iP_{\nu}HP_{\nu}\tau'}}{= \prod_{1 \leq \nu \leq |\mathcal{R}_{c}|}} \stackrel{e^{-iP_{\nu}HP_{\nu}\tau'}}{= \prod_{1 \leq \nu \leq |\mathcal{R}_{c}|} \stackrel{e^{-iH_{\nu}HP_{\nu}\tau'}}{= \prod_{1 \leq \nu \leq |\mathcal{R}_{c}|}} P_{\nu}e^{-iH\tau'}P_{\nu} \qquad (85)$$

$$\approx e^{-i(\sum_{C \in \mathcal{V}_{c}} H_{\text{diag}}^{C}(\gamma_{C}) + H_{\text{res}})\tau} = e^{-iH_{\text{res}}\tau} \prod_{C \in \mathcal{V}_{c}} e^{-iH_{\text{diag}}^{C}(\gamma_{C})\tau},$$

where $\mathcal{R}_c = \{PQ : P \in \mathcal{P}_c, Q \in \mathcal{Q}_c\} = \{P_{\nu}\}, \tau' = \tau/(2|\mathcal{R}_c|), \text{ and in } \approx \text{ we neglected all terms that are of order } \tau^3 \text{ or higher.}$

The number of Pauli operators needed to implement a step for a short time τ scale linearly with $|\mathcal{R}_c| = |\mathcal{P}|_c |\mathcal{Q}_c|$. Because, by Lemma 19,

$$|\mathcal{P}_c| = 4^{\chi_q} \le 4^{(\mathfrak{d}+1)(k-2)+1}, \quad |\mathcal{Q}_c| \le 2^k,$$
 (86)

we have

$$|\mathcal{R}_c| \le 4^{(\mathfrak{d}+1)(k-2)+k/2+1}.$$
 (87)

It is important to note that $|\mathcal{R}_c|$ is independent of the system size N.

Below we estimate how many Trotter steps are needed to make the actual dynamics close to limiting dynamics. The proof of this theorem is given in Section VI.

Theorem 20 (Number of Trotter steps needed). Assume that H is a low-intersection Hamiltonian defined in Definition 2, and $\mathcal{V} = \bigsqcup_{c \in [\chi]} \mathcal{V}_c$ is a coloring according to Lemma 5, $c \in [\chi]$, and $\gamma_C \in \{X, Y, Z\}^C$ for each $C \in \mathcal{V}_c$. Let $\mathcal{U}(\tau)$ be defined in (85), and let $\rho(t) = \mathcal{U}(\tau)^r \rho(0) (\mathcal{U}(\tau)^{\dagger})^r$ be the state of the quantum system at time t after being initialized in state $\rho(0)$. Then there exists $r_0 = \mathcal{O}(t^{3/2}/\varepsilon^{1/2})$ such that for any $r > r_0$, such that for any C and O_C supported on C, with $||O_C|| \leq 1$, we have

$$\left| \operatorname{tr}[(O_C \otimes I)\rho(t)] - \operatorname{tr}[O_C e^{-iH_{\operatorname{diag}}^C(\gamma_C)t} \rho_C e^{iH_{\operatorname{diag}}^C(\gamma_C)t}] \right| \le \varepsilon, \tag{88}$$

where $\rho_C = \operatorname{tr}_{[N] \setminus C} \rho(0)$.

In our Hamiltonian learning algorithm, we only need to ensure that the actual dynamics deviate from the limiting dynamics by a small constant. Therefore it suffices to choose $r = \mathcal{O}(\epsilon^{-3/2})$ in the above theorem (ϵ is the precision for Hamiltonian parameters, and ϵ^{-1} is the evolution time needed for robust phase estimation), as opposed to $r = \mathcal{O}(\epsilon^{-2})$ needed in the randomization approach. We summarize the costs of the Trotter-based approach in the following theorem

Theorem 21 (Learning many-body Hamiltonian by reshaping with Trotter formula). Assume that H is a low-intersection Hamiltonian defined in Definition 2. Then we can generate estimates $\{\hat{\lambda}_a\}$ for parameters $\{\lambda_a\}$ in (2), such that

$$\Pr[|\hat{\lambda}_a - \lambda_a| > \epsilon] < \delta \tag{89}$$

for all $a \in [M]$ with the following cost:

- 1. $\mathcal{O}(\epsilon^{-1}\log(\delta^{-1}))$ total evolution time;
- 2. $\mathcal{O}(\text{polylog}(\epsilon^{-1})\log(\delta^{-1}))$ number of experiments;
- 3. $\mathcal{O}(N\epsilon^{-3/2}\operatorname{polylog}(\epsilon^{-1})\log(\delta^{-1}))$ single-qubit Clifford gates.

Moreover, this algorithm is robust against SPAM error.

The SPAM-robustness follows in a similar way as in the proof of Theorem (13).

VI. DEVIATION FROM THE LIMITING DYNAMICS IN TROTTERIZATION

In this section we will prove Theorem 20. Following the discussion in Section IV, we only need to prove the following theorem, providing an error bound for the evolution of an arbitrary local operator in the Heisenberg picture.

Theorem 22. We assume that H is a low-intersection Hamiltonian as defined in Definition 2, let $\mathcal{U}(\tau)$ be as defined in (85), where the set of Pauli operators \mathcal{R}_c satisfies

$$\frac{1}{|\mathcal{R}_c|} \sum_{P \in \mathcal{R}_c} PHP = H_{\text{eff}}^C + H_{\text{env}}, \tag{90}$$

where H_{eff}^{C} is supported on a subsystem C ($|C|=\mathcal{O}(1)$) and H_{env} is supported on the rest of the system. Then

$$\left\| \left(\mathcal{U}(\tau)^{\dagger} \right)^r (O_C \otimes I) \mathcal{U}(\tau)^r - e^{iH_{\text{eff}}^C t} O_C e^{-iH_{\text{eff}}^C t} \otimes I \right\| = \mathcal{O}(t^3/r^2), \tag{91}$$

for any O_C supported on C satisfying $||O_C|| \le 1$. In particular, the constant in $\mathcal{O}(t^3/r^2)$ does not depend on the system size N or the number of terms M.

Proof. We rewrite the $\mathcal{U}(\tau)$ defined in (85) as $\mathcal{U}(\tau,0)$, and also write it as the unitary time evolution operator due to a time-dependent Hamiltonian:

$$\mathcal{U}(\tau,0) = \mathcal{T}e^{-i\int_0^\tau \widetilde{H}(s)\,ds},\tag{92}$$

where H(s) is a piecewise time-dependent Hamiltonian and is defined as follows: we divide the interval $[0,\tau]$ into $2|\mathcal{R}_c|$ sub-intervals, and one each sub-interval \widetilde{H} equals PHP with $P \in \mathcal{R}_c$ and then reverse the order.

Notice that, in order to prove (91), because the long time error grows linearly with respect to r thanks to the triangle inequality and the unitarity of both underlying dynamics, it is sufficient to bound the one-step error (i.e., the local truncation error using the terminology of numerical analysis [5])

$$\left\| \left(e^{iH_{\text{eff}}^C \tau} O_C e^{-iH_{\text{eff}}^C \tau} \right) \otimes I - \mathcal{U}(\tau, 0)^{\dagger} \left(O_C \otimes I \right) \mathcal{U}(\tau, 0) \right\| = \left\| T_{\text{eff}}(\tau) - T_{\text{tr}}(\tau) \right\|, \tag{93}$$

where

$$T_{\text{eff}}(\tau) = \left(e^{iH_{\text{eff}}^C \tau} O_C e^{-iH_{\text{eff}}^C \tau}\right) \otimes I, \quad T_{\text{tr}}(\tau) = \mathcal{U}(\tau, 0)^{\dagger} \left(O_C \otimes I\right) \mathcal{U}(\tau, 0). \tag{94}$$

We start by performing series expansion of both terms on the left-hand side in (93). By the Taylor's theorem, we have

$$e^{iH_{\rm eff}^C\tau}O_C e^{-iH_{\rm eff}^C\tau}$$

$$=O_C + i\tau[H_{\text{eff}}^C, O_C] - \frac{\tau^2}{2}[H_{\text{eff}}^C, [H_{\text{eff}}^C, O_C]] - i\int_0^\tau \frac{(\tau - s)^2}{2} e^{iH_{\text{eff}}^C s}[H_{\text{eff}}^C, [H_{\text{eff}}^C, O_C]]]e^{-iH_{\text{eff}}^C s} ds.$$

For the second term, a key observation is that

$$T_{\rm tr}(t) = \mathcal{T}e^{i\int_0^t \operatorname{ad}_{H(t-s)} ds} \left(O_C \otimes I\right). \tag{95}$$

To see this, denote $O_C \otimes I$ as O and $F(t,s) := \mathcal{U}(s,t)O\mathcal{U}(t,s)$, it follows from taking the derivative of F(t,s) with respect to s that

$$\partial_s F(s,t) = -i[H(s), F(s,t)] = -i \operatorname{ad}_{H(s)} F(s,t), \quad F(s=t,t) = O,$$

so that

$$\partial_s F(t-s,t) = i[H(t-s), F(t-s,t)] = i \operatorname{ad}_{H(t-s)} F(t-s,t), \quad F(t-s,t)|_{s=0} = O.$$

We now perform the Dyson series expansion to (95) and arrive at

$$T_{\text{tr}}(\tau) = \sum_{N=0}^{\infty} i^{N} \int_{0}^{\tau} dt_{1} \int_{0}^{t_{1}} dt_{2} \cdots \int_{0}^{t_{N-1}} dt_{n} \operatorname{ad}_{H(\tau-t_{1})} \circ \operatorname{ad}_{H(\tau-t_{2})} \circ \cdots \circ \operatorname{ad}_{H(\tau-t_{n})}(O)$$

$$= \sum_{N=0}^{\infty} i^{N} \int_{0}^{\tau} ds_{1} \int_{s_{1}}^{\tau} ds_{2} \cdots \int_{s_{N-1}}^{\tau} ds_{n} [H(s_{1}), [H(s_{2}), \cdots, [H(s_{n}), O], \cdots]].$$

Gathering terms of $\mathcal{O}(\tau^0)$, one has $O_C \otimes I$. The terms of $\mathcal{O}(\tau^1)$ read

$$i\int_0^\tau ds_1[H(s_1),O_C\otimes I]=i\left[\frac{\tau}{|\mathcal{R}_c|}\sum_{P\in\mathcal{R}_c}PHP,O_C\otimes I\right]=i\tau[H_{\text{eff}}^C,O_C]\otimes I.$$

The terms of $\mathcal{O}(\tau^2)$ are

$$\begin{split} & - \int_{0}^{\tau} ds_{1} \int_{s_{1}}^{\tau} ds_{2} [H(s_{1}), [H(s_{2}), O_{C} \otimes I] = -\frac{\tau^{2}}{4|\mathcal{R}_{c}|^{2}} \left[\sum_{j=1}^{2|\mathcal{R}_{c}|} H_{j}, \left[\sum_{l=j}^{|\mathcal{R}_{c}|} H_{l}, O_{C} \otimes I \right] \right] \\ & = -\frac{\tau^{2}}{4|\mathcal{R}_{c}|^{2}} \left(\left[\sum_{j=1}^{|\mathcal{R}_{c}|} H_{j}, \left[2 \sum_{l=1}^{|\mathcal{R}_{c}|} H_{l} - \sum_{l=1}^{j} H_{l}, O_{C} \otimes I \right] \right] + \left[\sum_{j=|\mathcal{R}_{c}|}^{2|\mathcal{R}_{c}|} H_{j}, \left[\sum_{l=1}^{j} H_{l}, O_{C} \otimes I \right] \right] \right) \\ & = -\frac{\tau^{2}}{2} [H_{\text{eff}}^{C}, [H_{\text{eff}}^{C}, O_{C}]] \otimes I, \end{split}$$

where we used the fact that H(s) is piece-wise constant, and we label its value on each piece as H_j so that $H_{j+|\mathcal{R}_c|} = H_{|\mathcal{R}_c|-j}$ for $1 \leq j \leq |\mathcal{R}_c|$. It can be seen that the first three terms of $T_{\rm tr}(\tau)$ match those of $T_{\rm eff}(\tau)$. For the terms with $j \geq 3$, we note that for each s, $\widetilde{H}(s) = PHP$ for some Pauli operator P, and $\widetilde{H}(s)$ therefore consists of Pauli operators that have exactly the same supports as those in H. Consequently, using the same argument as (61)-(62), each term can be bounded through

$$||[H(s_1), [H(s_2), \cdots, [H(s_n), O] \cdots]]|| \le j! (2(\mathfrak{d} + 1))^j.$$
 (96)

As a result the sum of these terms is bounded by $\mathcal{O}(\tau^3)$. Also note that the last term of (95) can be bounded by $4 \|H_{\text{eff}}^C\|^3 \tau^3/3$, where $H_{\text{eff}}^C = \mathcal{O}(1)$ as argued in the proof of Lemma 7. Therefore, we can conclude that

$$||T_{\text{eff}}(\tau) - T_{\text{tr}}(\tau)|| \le A_5 \tau^3$$

for some constant A_5 independent of the system size, and hence

$$\left\| \left(e^{iH_{\text{eff}}^C t} O_C e^{-iH_{\text{eff}}^C t} \right) \otimes I - \left(\mathcal{U}(\tau, 0)^{\dagger} \right)^r \left(O_C \otimes I \right) \left(\mathcal{U}(\tau, 0) \right)^r \right\| \le A_5 r \tau^3 = A_5 \frac{t^3}{r^2}, \tag{97}$$

which establishes the claim of this theorem.

VII. LOWER BOUND FOR LEARNING HAMILTONIAN FROM DYNAMICS

In this section, we present a fundamental lower bound on the total evolution time for any learning algorithm that tries to learn an unknown Hamiltonian from dynamics.

A. Model of quantum experiments

We consider a unitary U(t) parameterized by time t that implements e^{-iHt} for an unknown N-qubit Hamiltonian H. A learning agent can access U(t) by quantum experiments. We define a single ideal quantum experiment as follows. The definition resembles the formalism given in [6].

Definition 23 (A single ideal experiment). Given an unknown N-qubit unitary $U(t) = e^{-iHt}$ parameterized by time t. A single ideal experiment $E^{(0)}$ is specified by:

- 1. an arbitrary N'-qubit initial state $|\psi_0\rangle \in \mathbb{C}^{2^{N'}}$ with an integer $N' \geq N$,
- 2. an arbitrary POVM $\mathcal{F} = \{M_i\}_i$ on N'-qubit system,
- 3. an N'-qubit unitary of the following form,

$$U_{K+1}(U(t_K) \otimes I)U_K \dots U_3(U(t_2) \otimes I)U_2(U(t_1) \otimes I)U_1,$$
 (98)

for some arbitrary integer K, arbitrary evolution times $t_1, \ldots, t_K \in \mathbb{R}$, and arbitrary N'-qubit unitaries $U_1, \ldots, U_K, U_{K+1}$. Here I is the identity unitary on N' - N qubits.

A single run of $E^{(0)}$ returns an outcome from performing the POVM $\mathcal F$ on the state

$$U_{K+1}(U(t_K) \otimes I)U_K \dots U_3(U(t_2) \otimes I)U_2(U(t_1) \otimes I)U_1 |\psi_0\rangle.$$

$$\tag{99}$$

The evolution time of the experiment is defined as $t(E^{(0)}) \triangleq \sum_{k} |t_k|$.

The learning algorithm can adaptively choose each quantum experiment based on past measurement outcomes. We consider the quantum experiments to have a small unknown state preparation and measurement (SPAM) error. Given an initial state $|\psi_0\rangle$, the actual initial state being prepared on the quantum system is ρ_0 , which is equal to $|\psi_0\rangle\langle\psi_0|$ up to a small constant error η in the trace norm. Similarly, given a POVM $\mathcal{F} = \{M_i\}_i$, the actual POVM being measured is $\tilde{\mathcal{F}} = \{\tilde{M}_i\}_i$, where \tilde{M}_i is equal to M_i up to a small constant error η in the trace norm. A small SPAM error is always present in any quantum experiment. Measurement noises are particularly assured as measurements require the quantum system to interact with the macroscopic classical world, which often result in decoherence. A practically useful algorithm for characterizing and benchmarking quantum systems [4, 6–11] has to be robust against a small amount of SPAM error.

If a learning algorithm works for any small unknown SPAM error, then the learning algorithm must apply to experiments where only the measurement is subject to a small depolarizing noise η . We give a single experiment with measurement noise η in the following definition. The lower bound will be proved assuming access to the experiments with a small measurement noise $\eta = \Theta(1)$.

Definition 24 (A single experiment with measurement noise). A single experiment $E^{(\eta)}$ with measurement noise $\eta = \Theta(1)$ is specified by the same parameters as a single ideal experiment E^0 . Given the ideal POVM $\mathcal{F} = \{M_i\}_i$, the measurement outcome of $E^{(\eta)}$ is obtained by performing the noisy POVM $\mathcal{F}^{(\eta)} = \{(1-\eta)M_i + \eta \operatorname{tr}(M_i)(I/2^{N'})\}$ on the state

$$U_{K+1}(U(t_K) \otimes I)U_K \dots U_3(U(t_2) \otimes I)U_2(U(t_1) \otimes I)U_1 | \psi_0 \rangle$$
. (100)

The evolution time of the experiment is defined as $t(E^{(\eta)}) \triangleq \sum_{k} |t_k|$.

We formally define a learning algorithm with total evolution time T as follows.

Definition 25 (Learning algorithm with bounded total evolution time). Given $T > 0, 0.5 > \eta > 0$. A learning algorithm with total evolution time T and measurement noise η can obtain measurement outcomes from an arbitrary number of experiments $E_1^{(\eta)}, E_2^{(\eta)}, \dots$ as long as

$$\sum_{i} t(E_i^{(\eta)}) \le T. \tag{101}$$

The parameters specifying each experiment $E_i^{(\eta)}$ can depend on the measurement outcomes from previous experiments $E_1^{(\eta)}, \ldots, E_{i-1}^{(\eta)}$.

B. Learning task and lower bound

After defining the learning algorithm and the possible sets of experiments, we are ready to state the lower bound on the total evolution time required to learn an N-qubit Hamiltonian from dynamics. The theorem is stated as follows. This scaling matches that of our proposed learning algorithm.

Theorem 26. Given two integers N, M, two real values $\epsilon, \delta \in (0, 1)$, and a set $\{E_1, \ldots, E_M\} \subseteq \{I, X, Y, Z\}^{\otimes N} \setminus \{I^{\otimes N}\}$ of M Pauli operators. Consider any learning algorithm with a total evolution time T and a constant measurement noise $\eta \in (0, 0.5)$, such that for any N-qubit Hamiltonian $H = \sum_{a=1}^{M} \lambda_a E_a$ with unknown parameters $|\lambda_a| \leq 1$, after multiple rounds of experiments, the algorithm can estimate λ_a to ϵ -error with probability at least $1 - \delta$ for any $a \in \{1, \ldots, M\}$. Then

$$T \ge \frac{\log(1/2\delta)}{2\epsilon \log(1/\eta)} = \Omega\left(\frac{\log(1/\delta)}{\epsilon}\right). \tag{102}$$

Even when the measurement noise $\eta = 10^{-10}$, we still have $T \ge \log(1/2\delta)/(40\epsilon)$.

C. Proof of Theorem 26

The proof of the lower bound is separated into four parts. The first part in Section VII C1 reduces the learning problem to a binary distinguishing task. The second part in Section VII C2 provides an upper bound for the total variation (TV) distance between the distribution over measurement outcomes under a single experiment. The third part in Section VII C3 uses a learning tree representation described in [12, 13] and provides an upper bound for the total variation distance between distribution over the leaf nodes of the tree. The fourth part in Section VII C4 utilizes LeCam's two-point method to turn the TV upper bounds into a lower bound for the total evolution time.

1. Reduction

If a learning algorithm can achieve the original learning task considered in Theorem 26, then it could solve a simpler learning task, where the unknown Hamiltonian H can only be one of the following two choices. The unknown N-qubit Hamiltonian H is either ϵE_1 or $-\epsilon E_1$ with equal probability, where $E_1 \in \{I, X, Y, Z\}^{\otimes N} \setminus \{I^{\otimes N}\}$ is an N-qubit Pauli operator that is not an identity operator. We denote $U_{\pm}(t)$ to be the unitary corresponding to evolution under the two Hamiltonians. If there is a learning algorithm with a total evolution time at most T that succeeds in the learning task stated in Theorem 26, then we can use the learning algorithm to successfully distinguish between $\pm \epsilon E_1$ with probability at least $1-\delta$. Hence, a lower bound on T for this simpler learning task immediately implies a lower bound on T for the original learning task.

We can characterize the diamond distance between the two unitaries $U_{\pm}(t)$. For a unitary U, we consider $\mathcal{U}(\rho) = U\rho U^{\dagger}$ to be the corresponding quantum channel (CPTP map).

Lemma 27 (Diamond distance between $U_{\pm}(t)$). $\|\mathcal{U}_{+}(t) - \mathcal{U}_{-}(t)\|_{2} \leq 4\epsilon |t|$

Proof. The spectrum of $U_{+}(t)^{\dagger}U_{-}(t)$ is given by $e^{i2\epsilon t}$, $e^{-i2\epsilon t}$. From [14, 15], we have

$$\|\mathcal{U}_{+}(t) - \mathcal{U}_{-}(t)\|_{\diamond} = 2\sin(2\epsilon|t|) \tag{103}$$

if $2\epsilon |t| < \pi/2$, otherwise we have

$$\|\mathcal{U}_{+}(t) - \mathcal{U}_{-}(t)\|_{\diamond} = 2.$$
 (104)

In both cases, we have $\|\mathcal{U}_{+}(t) - \mathcal{U}_{-}(t)\|_{\diamond} \leq 4\epsilon |t|$.

2. TV upper bound for a single experiment

We begin by proving the upper bound on total variation distance for a single quantum experiment.

Lemma 28 (TV for one experiment). Given an unknown unitary U(t) equal to either $U_{+}(t)$ or $U_{-}(t)$, and a single experiment $E^{(\eta)}$ with measurement noise η specified by the following parameters,

- 1. an arbitrary N'-qubit initial state $|\psi_0\rangle \in \mathbb{C}^{2^{N'}}$ with an integer $N' \geq N$,
- 2. an arbitrary POVM $\mathcal{F} = \{M_i\}_i$ on N'-qubit system,
- 3. an N'-qubit unitary of the following form,

$$U_{K+1}(U(t_K) \otimes I)U_K \dots U_3(U(t_2) \otimes I)U_2(U(t_1) \otimes I)U_1,$$
 (105)

for some arbitrary integer K, arbitrary evolution times t_1, \ldots, t_K , and arbitrary N'-qubit unitaries $U_1, \ldots, U_K, U_{K+1}$. Here I is the identity unitary on N' - N qubits.

Let $p_{\pm}(i)$ be the probability of obtaining the measurement outcome i by performing $\mathcal{F}^{(\eta)} = \{(1-\eta)M_i + \eta \operatorname{tr}(M_i)(I/2^{N'})\}$ on the output state when $U(t) = U_{\pm}(t)$. Then

$$TV(p_+, p_-) \le (1 - \eta) \min(2\epsilon t(E^{(\eta)}), 1), \tag{106}$$

where $t(E^{(\eta)}) = \sum_{k=1}^{K} |t_k|$ is the total evolution time in this single experiment $E^{(\eta)}$.

Proof. We define $|\psi_{\pm}\rangle = U_K U_{\pm}(t_K) \dots U_3 U_{\pm}(t_2) U_2 U_{\pm}(t_1) U_1 |\psi_0\rangle$. By triangle inequality and telescoping sum, we have the following upper bound on the trace distance,

$$\||\psi_{+}\rangle\langle\psi_{+}| - |\psi_{-}\rangle\langle\psi_{-}|\|_{1} \le \sum_{k=1}^{K} \|U_{+}(t_{k}) - U_{-}(t_{k})\|_{\diamond} \le 4\epsilon \sum_{k=1}^{K} |t_{k}| = 4\epsilon t(E^{(\eta)}).$$
(107)

The second inequality follows from Lemma 27. We can now upper bound the total variation distance for the classical probability distribution when we measure the final state using the ideal POVM measurement $\mathcal{F} = \{M_i\}_i$,

$$\frac{1}{2} \sum_{i} |\langle \psi_{+} | M_{i} | \psi_{+} \rangle - \langle \psi_{-} | M_{i} | \psi_{-} \rangle| \le \frac{1}{2} |||\psi_{+} \rangle \langle \psi_{+}|| - |\psi_{-} \rangle \langle \psi_{-}|||_{1} \le 2\epsilon t(E^{(\eta)}). \tag{108}$$

Because the total variation distance is upper bounded by 1, we have

$$\frac{1}{2} \sum_{i} |\langle \psi_{+} | M_{i} | \psi_{+} \rangle - \langle \psi_{-} | M_{i} | \psi_{-} \rangle| \le \min(2\epsilon t, 1). \tag{109}$$

When we measure using the noisy POVM $\mathcal{F}^{(\eta)} = \{\tilde{M}_i = (1-\eta)M_i + \eta \operatorname{tr}(M_i)(I/2^{N'})\}$ instead of \mathcal{F} , the total variation distance between the measurement outcome distribution is

$$\frac{1}{2} \sum_{i} \left| \langle \psi_{+} | \tilde{M}_{i} | \psi_{+} \rangle - \langle \psi_{-} | \tilde{M}_{i} | \psi_{-} \rangle \right| \tag{110}$$

$$= \frac{1}{2} (1 - \eta) \sum_{i} |\langle \psi_{+} | M_{i} | \psi_{+} \rangle - \langle \psi_{-} | M_{i} | \psi_{-} \rangle| \le (1 - \eta) \min(2\epsilon t(E^{(\eta)}), 1). \tag{111}$$

By definition, we have $p_{\pm}(i) = \langle \psi_{\pm} | \tilde{M}_i | \psi_{\pm} \rangle$. Hence, $\text{TV}(p_+, p_-) \leq (1 - \eta) \min(2\epsilon t(E^{(\eta)}), 1)$, which is the total variation distance between the measurement outcome distribution over the two Hamiltonians under a single experiment.

3. TV upper bound for many experiments

To handle adaptivity in the choice of experiments, we consider the rooted tree representation \mathcal{T} described in [12, 13]. Each node in the tree corresponds to the sequence of measurement outcomes the algorithm has seen so far. We can also think of the node as the memory state of the algorithm. At each node v, the algorithm runs a single experiment $E_v^{(\eta)}$ with measurement noise η specified by

- 1. an arbitrary N'_v -qubit initial state $|\psi_{v,0}\rangle \in \mathbb{C}^{2^{N'_v}}$ with an integer $N'_v \geq N$,
- 2. an arbitrary POVM $\mathcal{F}_v = \{M_{v,i}\}_{i=1}^{L_v}$ with L_v outcomes on N'_v -qubit system,
- 3. an N'_v -qubit unitary of the following form,

$$U_{v,K_{v}+1}(U(t_{v,K_{v}}) \otimes I)U_{v,K_{v}} \dots U_{3,v}(U(t_{v,2}) \otimes I)U_{v,2}(U_{+}(t_{v,1}) \otimes I)U_{v,1},$$
 (112)

for some arbitrary integer K_v , arbitrary evolution times $t_{v,1}, \ldots, t_{v,K_v} \in \mathbb{R}$, and arbitrary N'_v -qubit unitaries $U_{v,1}, \ldots, U_{v,K+1}$. Here I is the identity unitary on $N'_v - N$ qubits.

Each experiment $E_v^{(\eta)}$ produces a measurement outcome $i \in \{1, \dots, L_v\}$, which moves the algorithm from the node v to one of its child node. At a leaf node ℓ , the algorithm stops. By considering the rooted tree representation and allowing the experiment to depend on each node in the tree, we cover all possible learning algorithm that can adaptively choose the experiment that it runs based on previous measurement outcomes.

For each node v on tree \mathcal{T} , we denote $p_{\pm}^{(\mathcal{T})}(v)$ to be the probability of arriving at the node v in the experiments when the unknown unitary $U(t) = U_{\pm}(t)$ and the algorithm begins from the root of \mathcal{T} . We can establish the following total variation upper bound.

Lemma 29 (TV for multiple experiments). Consider a rooted tree representation \mathcal{T} for a learning algorithm with total evolution time T and measurement noise $\eta \in (0, 0.5)$. We have

$$TV(p_+^{(\mathcal{T})}, p_-^{(\mathcal{T})}) \le 1 - \eta^{2\epsilon T}, \tag{113}$$

which is an upper bound for the total variation of the outcomes under multiple experiments.

Proof. For each node v, we give the following definitions,

- \mathcal{T}_v is the subtree with root v.
- $p_{\pm}^{(v)}$ is the distribution over the child nodes of v by considering the probability of moving from v to that child node under the unknown unitary $U_{\pm}(t)$.
- $p_{\pm}^{(\mathcal{T}_v)}$ is the distribution over the leaf nodes for subtree \mathcal{T}_v by considering the probability of ending at that leaf node starting from node v under the unknown unitary $U_{\pm}(t)$.
- $t^{(v)} \triangleq t(E_v^{(\eta)}) \ge 0$ is the evolution time for the single experiment $E_v^{(\eta)}$.
- $t(\mathcal{T}_v)$ is the maximum of the sum of the evolution time over all paths from root v of the subtree \mathcal{T}_v to a leaf node of \mathcal{T}_v ,

$$t(\mathcal{T}_v) = \max_{P: \text{path on } \mathcal{T}_v} \sum_{w \in P} t(E_w^{(\eta)}). \tag{114}$$

Because the total evolution time of the learning algorithm is upper bounded by T, the total evolution time of the full tree T satisfies $t(T) \leq T$.

We will prove this lemma by an induction over the subtree of \mathcal{T} . The inductive hypothesis is given as follows. For any subtree \mathcal{T}_v with root v,

$$1 - \text{TV}(p_{+}^{(\mathcal{T}_{v})}, p_{-}^{(\mathcal{T}_{v})}) \ge \eta^{2\epsilon t(\mathcal{T}_{v})}. \tag{115}$$

The base case is when v is a leaf node. At the leaf node ℓ , we have $TV(p_+^{(\mathcal{T}_\ell)}, p_-^{(\mathcal{T}_\ell)}) = 0$ and $t(\mathcal{T}_\ell) = 0$. Hence, the induction hypothesis holds.

To prove the inductive step, we define $\operatorname{child}(v)$ the be the set of child node of v and recall the following identity on two probability distributions p_{\pm} over a set \mathcal{X} ,

$$1 - TV(p_+, p_-) = \sum_{x \in \mathcal{X}} \min (p_+(x), p_-(x)).$$
 (116)

We can obtain a lower bound on the failure probability for the node v as follows,

$$1 - \text{TV}(p_+^{(\mathcal{T}_v)}, p_-^{(\mathcal{T}_v)}) \tag{117}$$

$$= \sum_{\ell \in \text{leaf}(\mathcal{T}_v)} \min \left(p_+^{(\mathcal{T}_v)}(\ell), p_-^{(\mathcal{T}_v)}(\ell) \right) \tag{118}$$

$$= \sum_{w \in \text{child}(v)} \sum_{\ell \in \text{leaf}(\mathcal{T}_w)} \min \left(p_+^{(v)}(w) p_+^{(\mathcal{T}_w)}(\ell), p_-^{(v)}(w) p_-^{(\mathcal{T}_w)}(\ell) \right)$$
(119)

$$\geq \sum_{w \in \text{child}(v)} \min \left(p_+^{(v)}(w), p_-^{(v)}(w) \right) \sum_{\ell \in \text{leaf}(\mathcal{T}_w)} \min \left(p_+^{(\mathcal{T}_w)}(\ell), p_-^{(\mathcal{T}_w)}(\ell) \right) \tag{120}$$

$$= \sum_{w \in \text{child}(v)} \min \left(p_{+}^{(v)}(w), p_{-}^{(v)}(w) \right) \left(1 - \text{TV} \left(p_{+}^{(\mathcal{T}_w)}, p_{-}^{(\mathcal{T}_w)} \right) \right)$$
(121)

$$\geq \left(1 - \text{TV}(p_{+}^{(v)}, p_{-}^{(v)})\right) \min_{w \in \text{child}(v)} \left(1 - \text{TV}\left(p_{+}^{(\mathcal{T}_w}, p_{-}^{(\mathcal{T}_w)}\right)\right). \tag{122}$$

We can apply the induction hypothesis on \mathcal{T}_w for $w \in \text{child}(v)$. This gives us

$$1 - \text{TV}(p_{+}^{(\mathcal{T}_{v})}, p_{-}^{(\mathcal{T}_{v})}) \ge \left(1 - \text{TV}(p_{+}^{(v)}, p_{-}^{(v)})\right) \eta^{2\epsilon t(\mathcal{T}_{w})}.$$
(123)

By definition, we have $t(\mathcal{T}_v) \geq t^{(v)} + t(\mathcal{T}_w)$ for any child node w of v, hence

$$1 - \text{TV}(p_{+}^{(\mathcal{T}_{v})}, p_{-}^{(\mathcal{T}_{v})}) \ge \eta^{2\epsilon \left(t(\mathcal{T}_{v}) - t^{(v)}\right)} \left(1 - \text{TV}(p_{+}^{(v)}, p_{-}^{(v)})\right). \tag{124}$$

From Lemma 28 that bounds the total variation distance for a single experiment, we have

$$TV(p_{+}^{(v)}, p_{-}^{(v)}) \le (1 - \eta) \min(2\epsilon t^{(v)}, 1).$$
(125)

Hence, we can obtain

$$1 - \text{TV}(p_{+}^{(\mathcal{T}_{v})}, p_{-}^{(\mathcal{T}_{v})}) \ge \eta^{2\epsilon \left(t(\mathcal{T}_{v}) - t^{(v)}\right)} \left(1 - (1 - \eta) \min(2\epsilon t^{(v)}, 1)\right)$$
(126)

$$\geq \eta^{2\epsilon \left(t(\mathcal{T}_v) - t^{(v)}\right)} \eta^{\min(2\epsilon t^{(v)}, 1)} \tag{127}$$

$$\geq \eta^{2\epsilon \left(t(\mathcal{T}_v) - t^{(v)}\right)} \eta^{2\epsilon t^{(v)}} = \eta^{2\epsilon t(\mathcal{T}_v)}. \tag{128}$$

The second inequality uses $1-(1-\eta)x \geq \eta^x$ for any $\eta \in (0,0.5)$ and $x \in [0,1]$, which follows from the convexity of $f(x) = \eta^x - 1 + (1 - \eta)x$ and the fact that f(0) = f(1) = 0. We have proved the inductive step.

Using induction and the fact that $t(\mathcal{T}) \leq T$, we have

$$TV(p_{+}^{(\mathcal{T})}, p_{-}^{(\mathcal{T})}) \le 1 - \eta^{2\epsilon T},\tag{129}$$

which is the claimed result.

4. Lower bound from TV upper bound

From the reduction step in Section VII C 1, for any learning algorithm with a total evolution time at most T that succeeds in the learning task stated in Theorem 26, we can use the learning algorithm to successfully distinguish between $U_+(t)$ with probability at least $1-\delta$. By the construction of the rooted tree representation \mathcal{T} , after the multiple experiments, the only information the learning algorithm can access corresponds to a leaf node of the tree \mathcal{T} . Hence, if the learning algorithm can distinguish between $U_{\pm}(t)$, then it can distinguish between the two probability distributions $p_{+}^{(\mathcal{T})}, p_{-}^{(\mathcal{T})}$ with probability at least $1 - \delta$.

Using LeCam's two point method, if there is an algorithm that can distinguish the two probability distributions

 $p_{+}^{(\mathcal{T})}, p_{-}^{(\mathcal{T})}$ with probability at least $1 - \delta$, then $1 - 2\delta \leq \text{TV}(p_{+}^{(\mathcal{T})}, p_{-}^{(\mathcal{T})})$. Thus,

$$2\delta \ge \eta^{2\epsilon T} \Longleftrightarrow T \ge \frac{\log(1/2\delta)}{2\epsilon \log(1/\eta)}.$$
 (130)

Recalling that $\eta \in (0, 0.5)$ is a constant close to 0, we have

$$T = \Omega\left(\frac{\log(1/\delta)}{\epsilon}\right). \tag{131}$$

We have thus established Theorem 26.

^[1] J. Haah, R. Kothari, and E. Tang, Optimal learning of quantum hamiltonians from high-temperature gibbs states, arXiv preprint arXiv:2108.04842 (2021).

^[2] E. Campbell, Random compiler for fast hamiltonian simulation, Physical review letters 123, 070503 (2019).

^[3] C.-F. Chen, H.-Y. Huang, R. Kueng, and J. A. Tropp, Concentration for random product formulas, PRX Quantum 2.

^[4] S. Kimmel, G. H. Low, and T. J. Yoder, Robust calibration of a universal single-qubit gate set via robust phase estimation, Physical Review A **92**, 062315 (2015).

^[5] R. J. LeVeque, Finite difference methods for ordinary and partial differential equations: steady-state and time-dependent problems (SIAM, 2007).

^[6] H.-Y. Huang, S. T. Flammia, and J. Preskill, Foundations for learning from noisy quantum experiments, arXiv preprint arXiv:2204.13691 (2022).

^[7] E. Knill, D. Leibfried, R. Reichle, J. Britton, R. B. Blakestad, J. D. Jost, C. Langer, R. Ozeri, S. Seidelin, and D. J. Wineland, Randomized benchmarking of quantum gates, Physical Review A 77, 012307 (2008).

^[8] E. Magesan, J. M. Gambetta, and J. Emerson, Scalable and robust randomized benchmarking of quantum processes, Physical review letters **106**, 180504 (2011).

^[9] A. Erhard, J. J. Wallman, L. Postler, M. Meth, R. Stricker, E. A. Martinez, P. Schindler, T. Monz, J. Emerson, and R. Blatt, Characterizing large-scale quantum computers via cycle benchmarking, Nature communications 10, 1 (2019).

^[10] R. Harper, S. T. Flammia, and J. J. Wallman, Efficient learning of quantum noise, Nature Physics 16, 1184 (2020).

^[11] A. Elben, S. T. Flammia, H.-Y. Huang, R. Kueng, J. Preskill, B. Vermersch, and P. Zoller, The randomized measurement toolbox, arXiv preprint arXiv:2203.11374 (2022).

- [12] H.-Y. Huang, M. Broughton, J. Cotler, S. Chen, J. Li, M. Mohseni, H. Neven, R. Babbush, R. Kueng, J. Preskill, et al., Quantum advantage in learning from experiments, Science 376, 1182 (2022).
- [13] S. Chen, J. Cotler, H.-Y. Huang, and J. Li, Exponential separations between learning with and without quantum memory, in 2021 IEEE 62nd Annual Symposium on Foundations of Computer Science (FOCS) (IEEE, 2022) pp. 574–585.
- [14] I. Nechita, Z. Puchała, L. Pawela, and K. Życzkowski, Almost all quantum channels are equidistant, Journal of Mathematical Physics 59, 052201 (2018).
- [15] J. Watrous, The theory of quantum information (Cambridge university press, 2018).